IFE/KR/E – 2008/004

LOCA testing of high burnup PWR fuel in the HBWR. Additional PIE on the cladding of the segment 650-5.

	KJELLER	HALDEN	open
Address	NO-2027 Kjeller, Norway	NO-1751 Halden, Norway	
Telephone	+47 63 80 60 00	+47 69 21 22 00	
Telefax	+47 63 81 xx xx	+47 69 21 22 01	

Report number	Date
IFE/KR/E-2008/004	2008-04-11
Report title and subtitle LOCA testing of high burnup PWR fuel in the HBWR. Additional PIE on the cladding of the segment 650-5.	**Number of pages** 35
Project/Contract no. and name Contract ML080150003	**ISSN** 0333-2039
Client/Sponsor Organisation and reference NRC/RES	**ISBN** 978-82-7017-704-2 (printed) 978-82-7017-705-9 (electronic)

Abstract

IFA-650.5, a test with pre-irradiated fuel in the Halden Project LOCA test series, was conducted on October 23rd, 2006. The fuel rod had been used in a commercial PWR and had a high burnup, 83 MWd/kgU. Experimental arrangements of the fifth test were similar to the preceding LOCA tests. The peak cladding temperature (PCT) level was higher than in the third and fourth tests, 1050 °C. A peak temperature close to the target was achieved and cladding burst occurred at ~750 ^{o}C. Within the joint programme framework of the Halden Project PIE was done, consisting of gamma scanning, visual inspection, neutron-radiography, hydrogen analysis and metallography / ceramography.
An additional extensive PIE including metallography, hydrogen analysis, and hardness measurements of cross-sections at seven axial elevations was done. It was completed to study the high burnup and LOCA induced effects on the Zr-4 cladding, namely the migration of oxygen into the cladding from the inside surface, the cladding distension, and the burst.

Keywords: Zr-4 nuclear fuel cladding, high temperature oxidation, mechanical properties, LOCA

	Name	Date	Signature
Author(s)	B.C.Oberländer M.Espeland H.K.Jenssen	2008-04-21	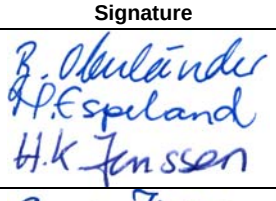
Reviewed by	E.Kolstad	2008-04-24	
Approved by	B.C.Oberländer	2008-04-25	

Contents

.

1 Introduction

IFA-650.5[1], the third test with pre-irradiated fuel in the Halden Project LOCA test series, was conducted on October 23rd, 2006. The fuel was provided by Framatome, ANP. The fuel rod had been used in a commercial PWR and had a high burnup, 83 MWd/kgU. Experimental arrangements of the fifth test were similar to the preceding LOCA tests. The peak cladding temperature (PCT) level in the fifth LOCA test was higher than in the third and fourth tests, 1050 °C. A peak temperature close to the target was achieved and cladding burst occurred at ~750 ^{o}C. Within the joint programme framework of the Halden Project PIE was done, consisting of gamma scanning, visual inspection, neutronradiography, and metallography/ceramography, as reported in IFE/KR/F-2008/064[2].

The additional extensive PIE included metallography, hydrogen analysis, and hardness measurements of cross-sections at seven axial elevations. It was completed to study, to measure and quantify the burnup and LOCA induced effects on the Zr-4 cladding, namely the migration of oxygen into the cladding from the inside surface, the heat treatment effect of the cladding microstructure e.g. grain size and grain morphology - alpha layer, the cladding mechanical properties e.g. cladding distension (hoop strain), wall thickness reduction and crack opening.

2 Experimental

The 83 MWd/kgU, high burnup rod segment reached a PCT of 1050 °C in the LOCA test. The rod segment was of 3.5 % enriched UO_2 fuel and a Zr-4 cladding with an outer diameter (OD) liner of the following composition Sn:0.84%, Fe:0.29%, Cr:0.17%, O:0.13%, and some low levels (ppm) of other elements, such as Al, Hf, C, Si, etc. Reference PIE data on the cladding were provided by Framatome.

PIE on the rod segment cladding after the LOCA test started with gamma scanning, visual inspection and neutron-radiography. Based on the NDT results destructive PIE included metallography and hydrogen analysis in rod cross-sections from 7 axial elevations. The total hydrogen content in the cladding was measured in axial rod elevations next to the metallography samples. Sampling locations on the 650-5 segment were indicated in the neutronradiograph in Fig.3.

3 Results

NDT PIE gave an overview on the LOCA induced disintegration state of cladding and fuel.

---

[1] **HP-1222** LOCA experiment. Initial results from the fifth test (IFA-650.5)

[2] **B.C.Oberländer, M.Espeland, H.K.Jenssen,** " PIE of the high burnup PWR segment 650-5 after LOCA testing in the HBWR", IFE/KR/F-2008/064 of 2008-04-11 (limited).

3.1 Gamma scanning

Gamma scanning gave evidence of a failure and cladding distension of the rod segment well below the lower end TC, as documented in Fig. 1. Cladding distension and burst was found 7-8 cm above the lower end active fuel stack.

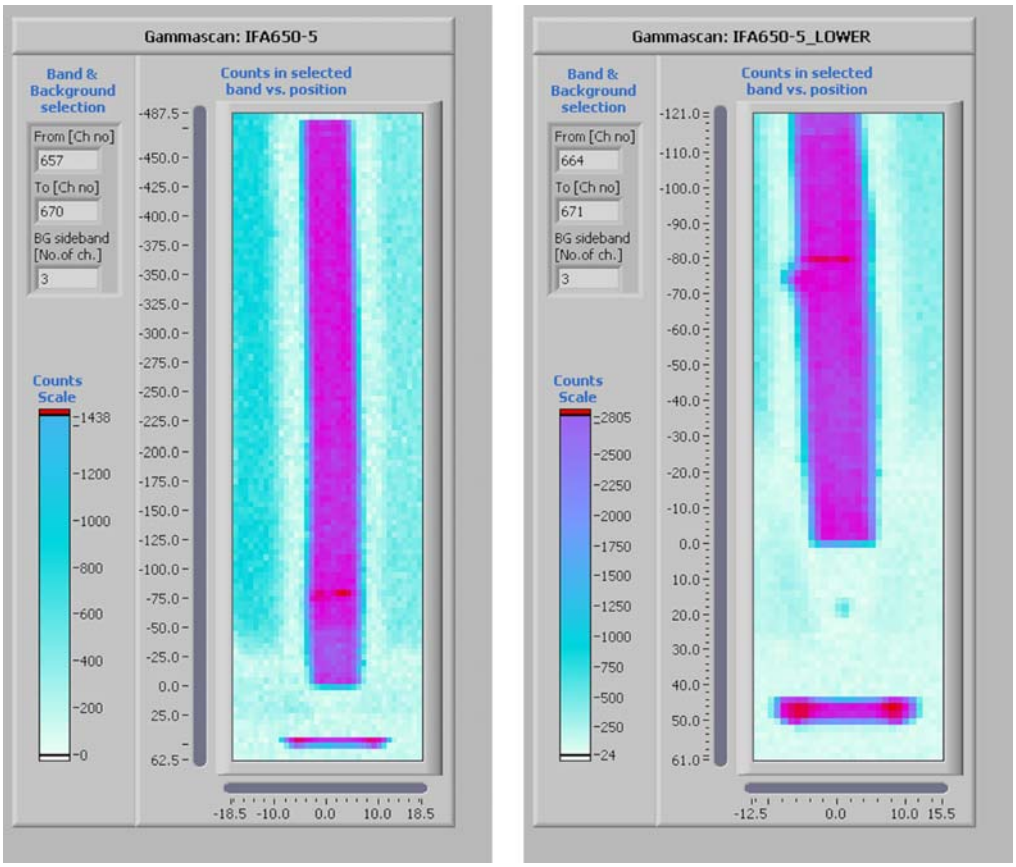

Failure and ballooning well below the lower TC

Fig. 1 Gamma scanning

3.2 Visual examination

Visual examination was made in two orientations, namely 0° and 90°. As presented in Fig. 2 rod 650-5 showed LOCA induced cladding distension and burst at 7-8 cm above the lower end active fuel stack. The burst is narrow and about 1 cm long. The defect occurred well below the lower cladding thermocouple. The cladding of the high burn-up (83 MWd/kg) PWR rod from which the segment for 650-5 was taken, had an intact, continuous 70-80 micrometer thick oxide on the outer diameter and a hydrogen content of 650 ppm, as reported from pre-test reference PIE. After the LOCA experiment visual examination showed white cracks in the thick outer surface oxide, due to the diameter increase of the cladding. The cracks in the thick surface oxide propagated in longitudinal direction and were visible in the clad oxide between the start of the active fuel stack and up to the axial elevation of about +20 cm. The white oxide cracks, however, were mainly seen in the same angular orientation as the burst, namely around 0°.

Fig.2 Visual inspection

3.3 Neutronradiography

Due to safety reasons the zone with ballooning and burst had to be covered prior to *neutronradiography*. The neutronradiographs showed creep of the cladding diameter in axial direction between the elevation of the start of active fuel stack and axial elevation +22 cm measured from the lower end. In the clad creep range no pellet-pellet interfaces are seen on the neutron-radiographs, see Fig. 3. The neutronradiographs gave evidence of fuel fragmentation and fragmentation in this zone. Above the axial elevation of +22 cm and all way towards the upper end of the active fuel stack the neutronradiographs showed whole pellets and clear pellet-pellet interfaces.

Sampling locations for destructive PIE were at 95mm, 120mm, 150mm, 184mm, 230mm, 470mm, and 517mm measured from the lower end of the rod.

Fig. 3 Neutronradiography

3.4 NDT-PIE related fuel and cladding diameter profiles and cutting plans for further destructive PIE

Diameter measurements, based on the visual inspection and neutronradiography were made to estimate the LOCA induced fuel diameter increase and the cladding distension. The results from the NDT observations and measurements were summarized in Fig. 4. Non-destructive PIE showed asymmetric cladding diameter increase with respect to the total axial length of the rod. In the lower end of the rod the cladding diameter increased steeply and rapidly to its maximum and burst. Burst of the cladding occurred without dramatic cladding distension / plastic deformation of the rod. In the balloon and burst zone the LOCA induced rod diameter increased from 10.8mm to 11.5mm in the upper and to 12.5mm in the lower part of the rod. Compared to the cladding in 650-4 the cladding of 650-5 showed a rather stiff and brittle behaviour. However, the low ductility was as expected due to the high burnup and high hydrogen content of the 650-5 cladding.

The axial fuel diameter variations assessed from neutronradiographs showed in the area with fuel fragmentation a diameter increase from 9.8 to 10.5mm below the clad burst, from there, the fuel diameter slope decreases slowly in the zone with fuel fragmentation to about 9.2mm in the middle

of the active fuel stack. From there and to the end of the active fuel stack the pellet-pellet interfaces were seen clearly in the neutronradiographs and the fuel diameter varied between 9.5 and 10.0mm.

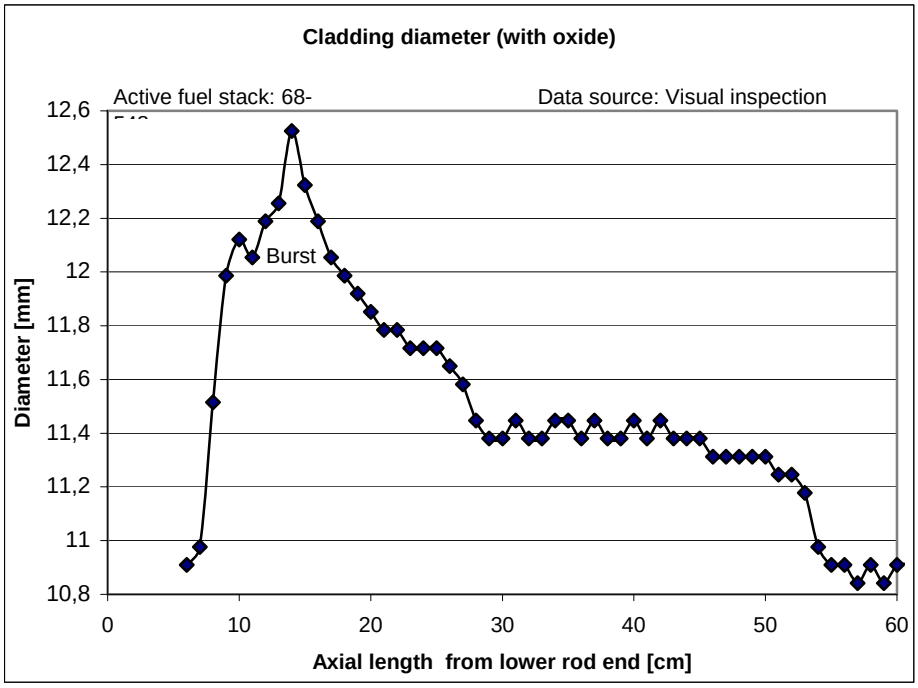

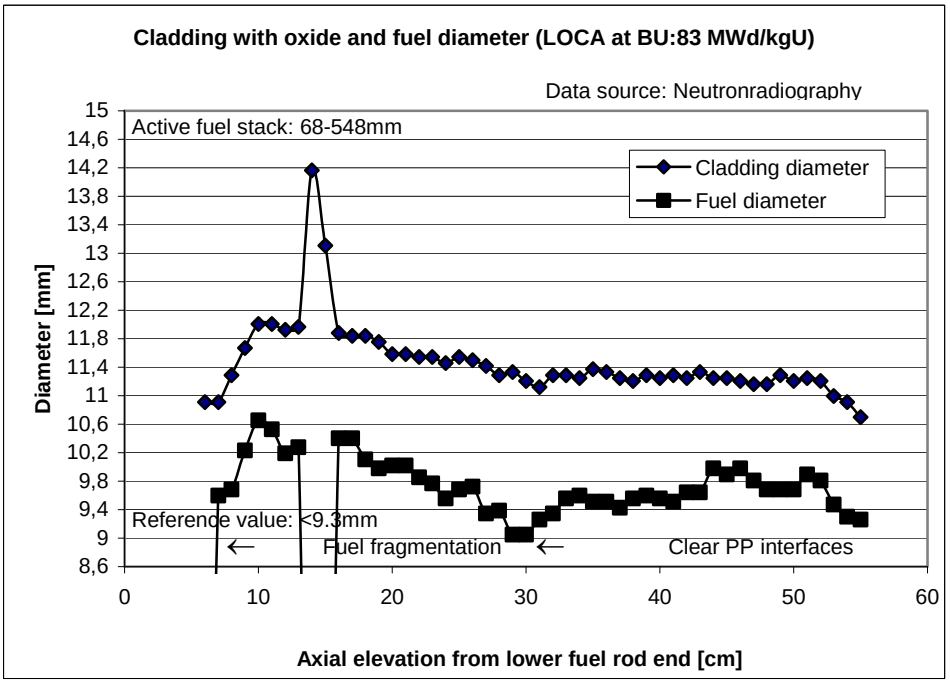

Fig.4. Diameter and cladding distension data are based on NDT-PIE. The LOCA induced cladding defect/burst is in the lower part of the rod and well below the lower cladding TC.

3.5 Metallography

3.5.1 Details of the cladding: Outer and inner surface oxides, grain morphology, alpha layer, hydrides, profiles on hydrogen content, hardness, and cladding distension

High temperature cladding corrosion effects were studied, e.g. the oxidation of the inner and outer cladding diameter and the hydriding of the cladding.

Oxide layer on cladding outer diameter. The pre-test reference PIE suggested an oxide thickness of the rod prior to segmenting and refabrication of 70-80 micrometers. Fig. 5a and b gives PIE details on the cladding oxide after the LOCA test. The measured thickness of the continuous oxide on the outer surface of the cladding (OD oxide) was about 70 μm, whereof the LOCA induced oxide growth was about 11μm as measured in the TC support (470 mm) location. Here, the oxide was ground off prior to the LOCA test. Other locations showing the LOCA induced oxide growth were found below radial oxide cracks, as shown in Fig. 5a. The lower oxide thickness found in this PIE compared to the reference PIE data can be explained by the different measuring locations on the original fuel rod.

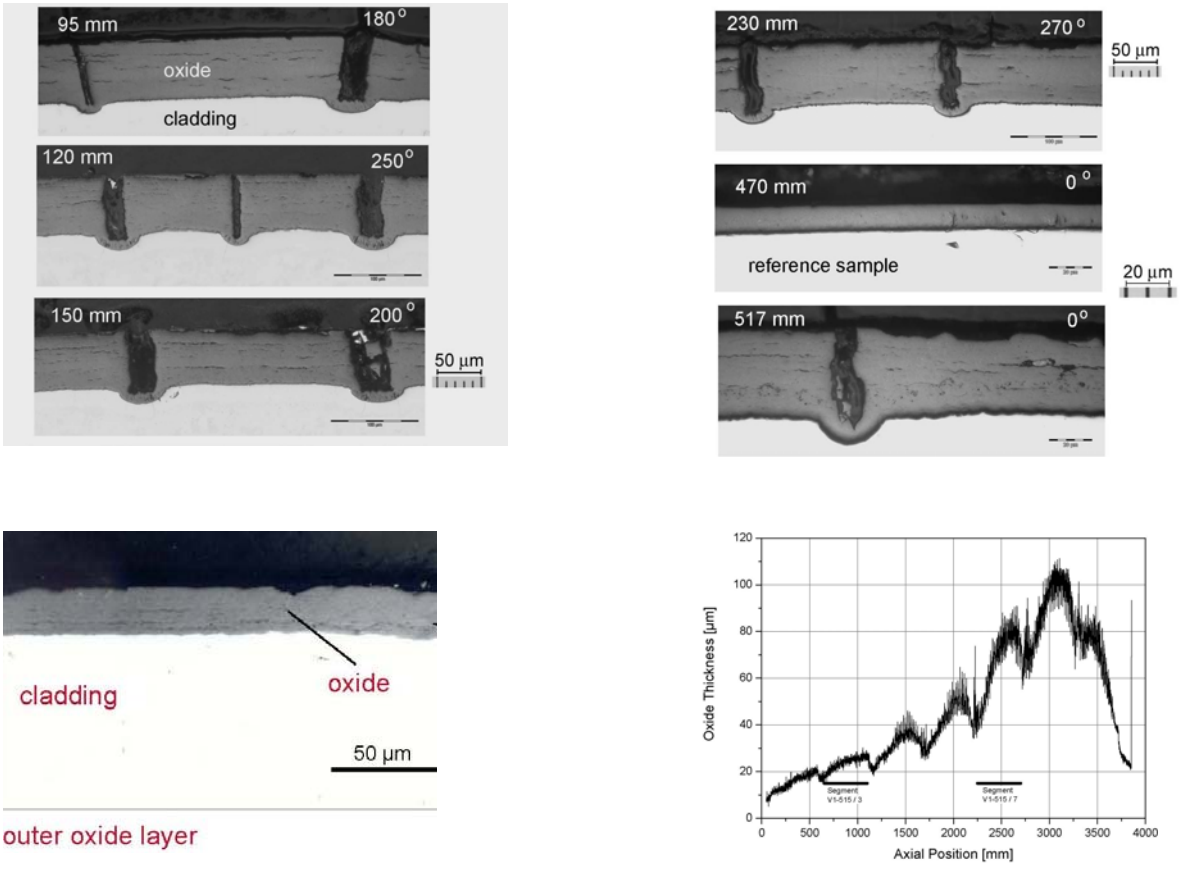

Fig. 5a Oxide layer morphology. The continuous oxide layer on the cladding OD showed radial cracks and a LOCA induced oxide growth below the radial cracks of about 11μm (upper row). Pre-test reference PIE (lower row).

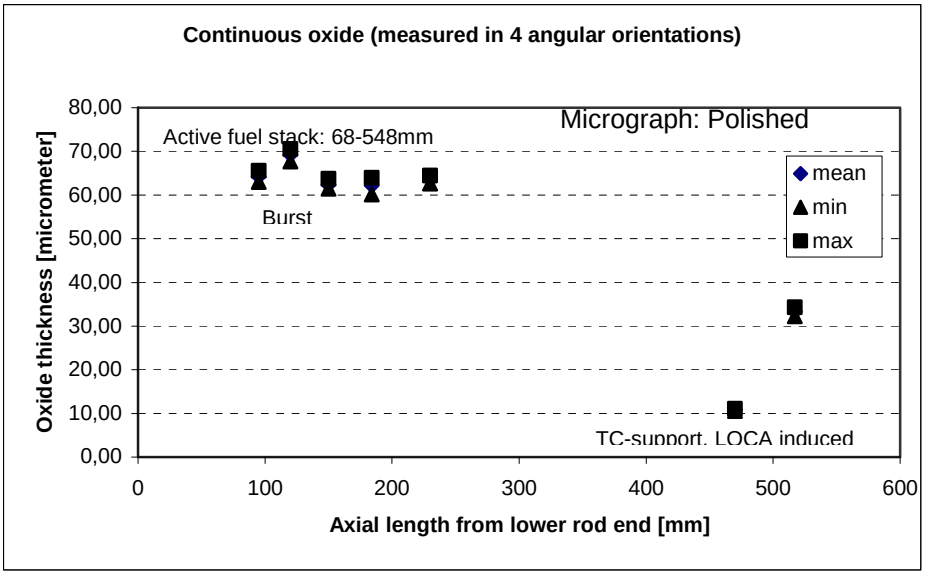

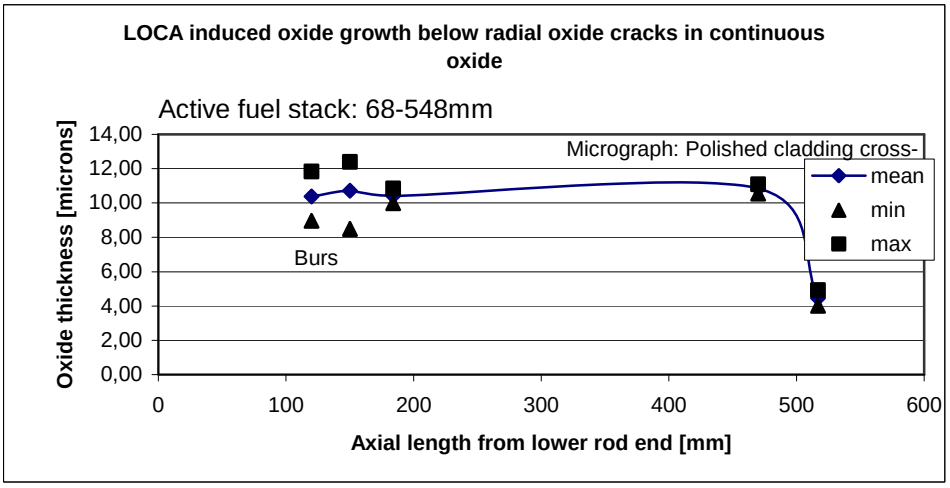

Fig. 5b Measured data for the continuous oxide and the LOCA induced oxide growth (11 μm)

Grain morphology of the cladding. The effect of the LOCA test induced heat treatment on the cladding microstructure e.g. cladding grain size and grain morphology was studied in optical microscopy and polarised light. Metallography revealed as expected and as a result of the temperature excursion above the alpha/beta phase transition temperature a grain growth with former β grains and a Widmanstätten structure. Typically, the grain-size was in the range of 40μm. Further, the cladding had an alpha layer with smaller grains at the outer (OD) and inner (ID) cladding diameter. The results of the cladding microstructure study in are documented in Fig. 6 a and b.

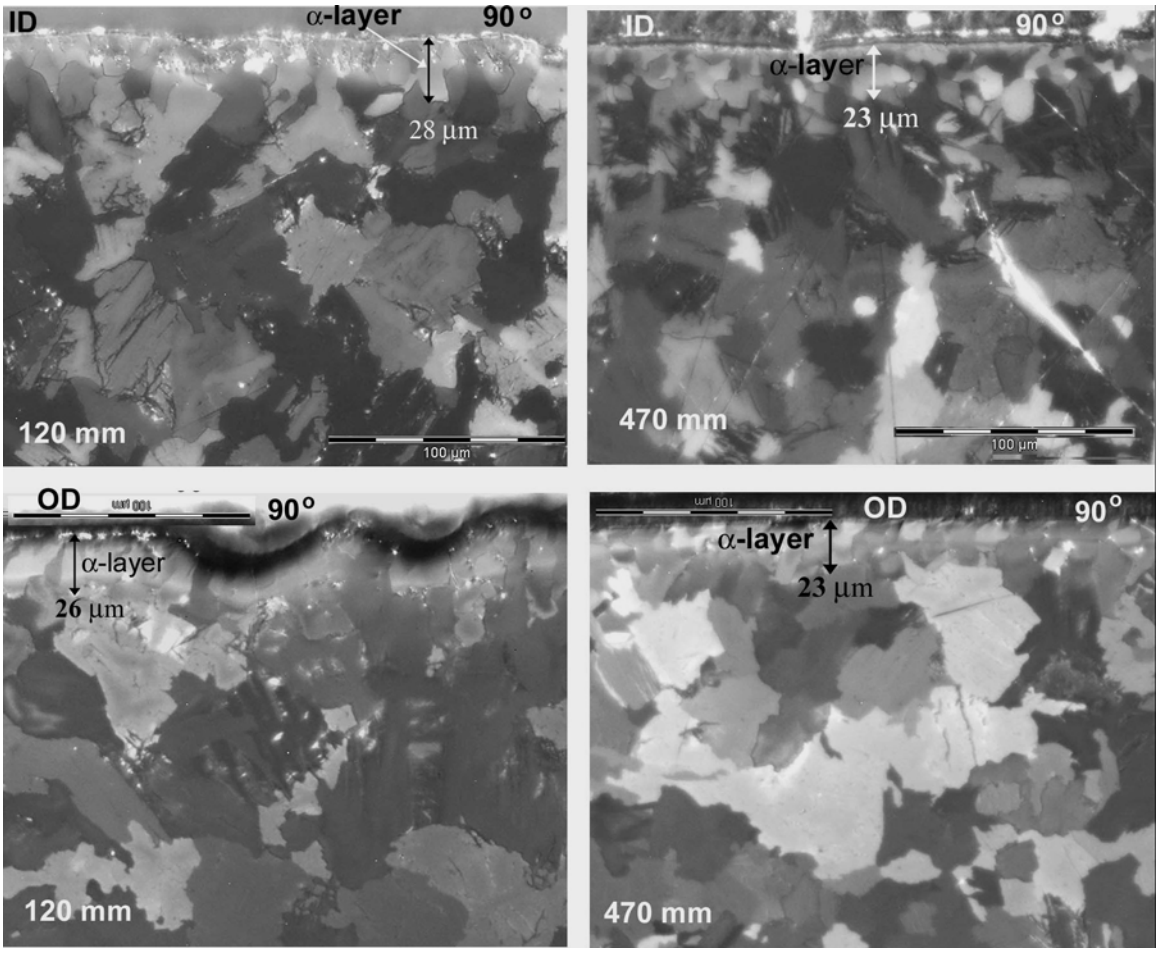

Fig. 6a The grain morphology study revealed grain growth with Widmanstätten structure and an OD and ID alpha layer with smaller grains.

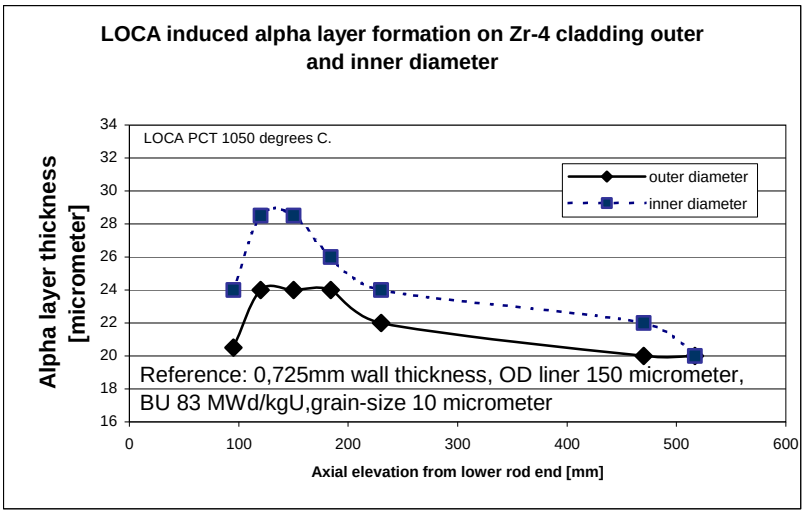

Fig. 6b Axial profile of the thickness of the alpha layer on the Zr-4 cladding (OD and ID).

Alpha layer: Oxygen, which caused alpha layer formation and cladding embrittlement, might enter from the inside diameter (ID) as well as from the outside diameter (OD) of the cladding on high-burnup fuel. On the cladding outer and inner wall a LOCA induced 20-30μm thick, oxygenrich, hard and brittle alpha layer as shown in Fig. 6 was found. The hard and brittle alpha layer is slightly wider on the inner diameter (ID) compared to the outer (OD) and the alpha layer is wider in the max balloon and burst area (OD:24 and ID:29 μm) compared to the upper part of the rod at 470 mm (OD:20 and ID:22 μm), see also Table 1 and Figs 3.5.18 through 3.5.24 in the Appendix.

Table 1 Alpha layer on cladding outer (OD) and inner (ID) surface. Thickness measurements *

Axial position	**OD α-layer (μm) 90^0**	**OD α-layer (μm) 270^0**	**ID α-layer (μm) 90^0**	**ID α-layer (μm) 270^0**	**Mean thickness (μm) OD / ID**
95 (MC1)	22	19	24	23,5	21 / 24
120 (MC2)	23,5	25	27,5	29,5	24 / 28,5
150 (MC3)	29	19,5	29	28	24 / 28,5
184 (MC4)	25	23	25	28	24 / 26,5
30 (MC5)	23	21,5	24	24,5	22 / 24
470 (MC6)	21,5	19	23,5	21	20 / 22
517 (MC7)	20	20	20	21	20 / 20,5

* 2-3 measurements per orientation on OD and ID

The source of oxygen in the upper elevations is assumed to be coming from the bonded fuel. 470 mm is at the top of the fuel stack, fairly close to the plenum above the segment and filled with argon, and 517 mm is even higher up. In the LOCA test IFA-650.5 it took a long time to empty the plenum, 1-1.5 min due to poor axial communication down the segment. The tight crack was about 7-8 cm from the bottom. A spray system was used above 800 °C in the test, but the steam produced would not be able to reach the inner, upper part of the segment and give cause for the inner diameter alpha layer formation. It is unlikely. We have data supporting this from test IFA-650.2 with fresh pellet (and open gap). PCT in that test was 1050 °C and the cladding ballooned and failed with a wide opening somewhat below the axial mid-plane of the segment. The spray system was applied here too. The measured oxide thickness was about 24-25 microns at the outside in the top part of the rod, at the elevation of the upper clad TCs, and very close to predictions, but zero or very small at the inside and at the same axial elevation.

Hydrogen analysis and hydride distribution. The cladding hydrogen content was given in the reference PIE with 650 ppm prior to LOCA. The total hydrogen content in the cladding was measured in 7 axial rod elevations. The sampling locations for hydrogen were next to the metallography samples. Hydrogen analysis was done using 2 mm high ring-samples. For experimental reasons the rings were subdivided into four ca. 50 mg samples, then cleaned and carefully dried in order to prevent contamination by foreign hydrogen. The analysis, based on a melt extraction method, was performed with an ELTRA OH-900 hydrogen analyzer. In the process

hydrogen released from the totally melted sample was carried away by the carrier gas, Argon. The hydrogen concentration was determined from changes in gas thermal conductivity, measured by a thermal conductivity detector. Accuracy of method is ± 1% of hydrogen content. The average H_2-content in each ring is equal to the weighed average of the H_2-content in the four samples.

Micrographs showing the typical distribution, orientation, and concentration of hydrides in a cross-section from the balloon zone, accompanied by a plot of the measured data on the hydrogen content of the samples examined were presented graphically in Fig.7.

Fig. 7 shows typically arbitrary oriented hydrides in the Widmanstätten structure of the cladding. The graph in Fig. 7 represents the hydrogen content measured along the axial length of the rod. LOCA induced hydrogen uptake phenomena can be derived from the axial hydrogen content profile. From the hydrogen data the following can be stated:

Remarkable is a higher hydrogen content analysed in the samples from the balloon zone in the lower part of the rod, than elsewhere. Actually, the axial profile for hydrogen has the same shape and characteristics as the LOCA induced axial profile for the cladding diameter.

Further, with respect to the hydrogen concentration distribution as function of the angular orientation in the cladding a scatter of the measured values as function of the angular orientations was observed. A significantly larger scatter/spread was observed for the hydrogen data from the samples from the balloon zone than for the data from the samples located elsewhere in the rod. This means in the balloon zone a larger variation in the hydrogen uptake in the cladding circumference was found than elsewhere in the cladding.

Mechanical properties of the cladding – Hardness, Cladding distension (hoop strain), wall thickness reduction and crack opening

Hardness: Series of hardness measurements in the cladding radii on etch polished cross-sections were done, namely below the burst opening (158 mm) and well above the burst opening (466 mm). The hardness indents were done by a Vickers diamond indenter [HV0.05] and a load of 50 g. The hardness of the high burnup, LOCA tested Zr-4 cladding showed after a temperature excursion to 1050°C in most of the cladding radius hardness values within 170 and 200 $HV_{0.05}$. Higher values were found in the alpha layer. The alpha layers were observed at the cladding outer ($520HV_{0.05}$) and inner surface ($420HV_{0.05}$). The measured hardness values are listed in Table 2 and the hardness profile and the respective cladding radii are shown in Fig. 8 and the Appendix.

The hardness profiles, namely from the cladding outer to the cladding inner surface showed a slight asymmetry. The asymmetry of the hardness values is affected by the 150 μm thick liner on the cladding OD.

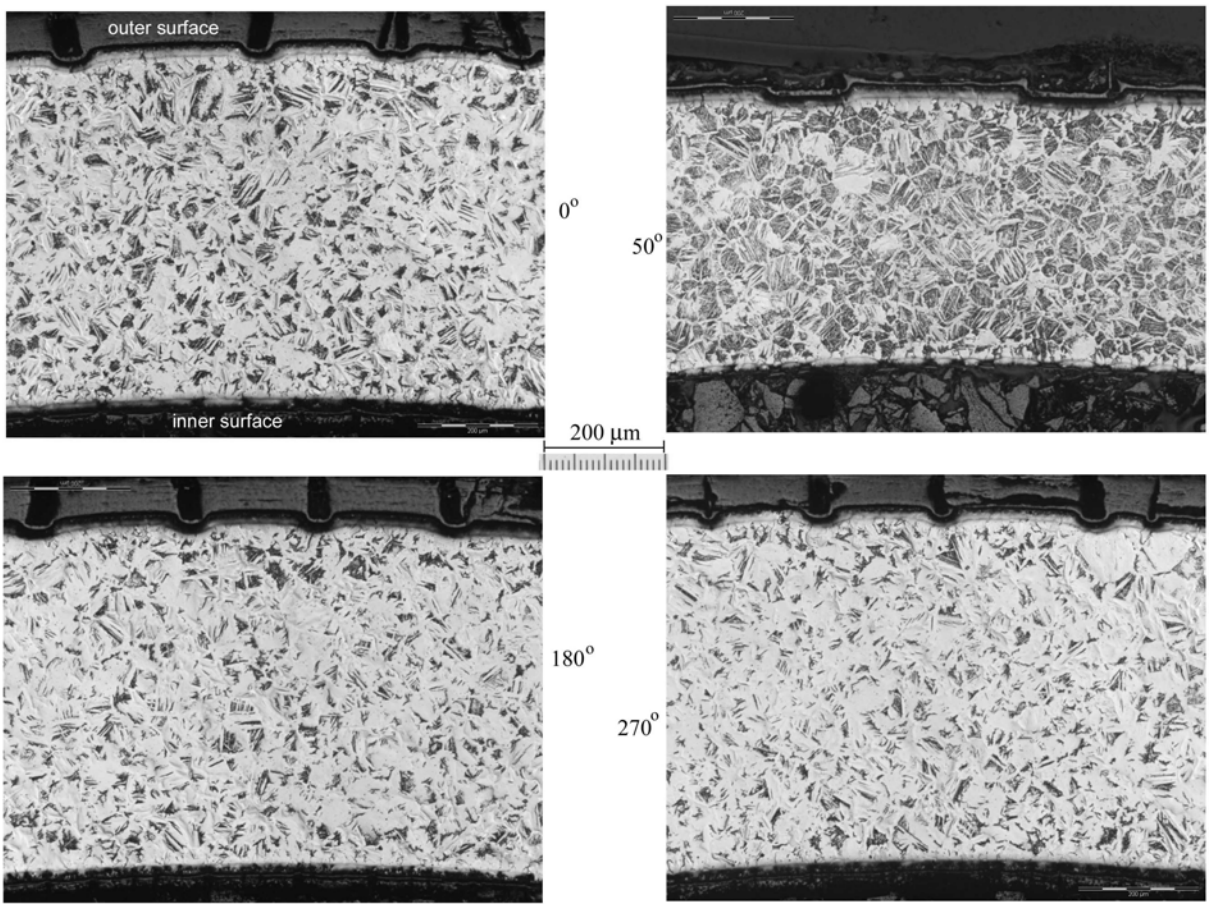

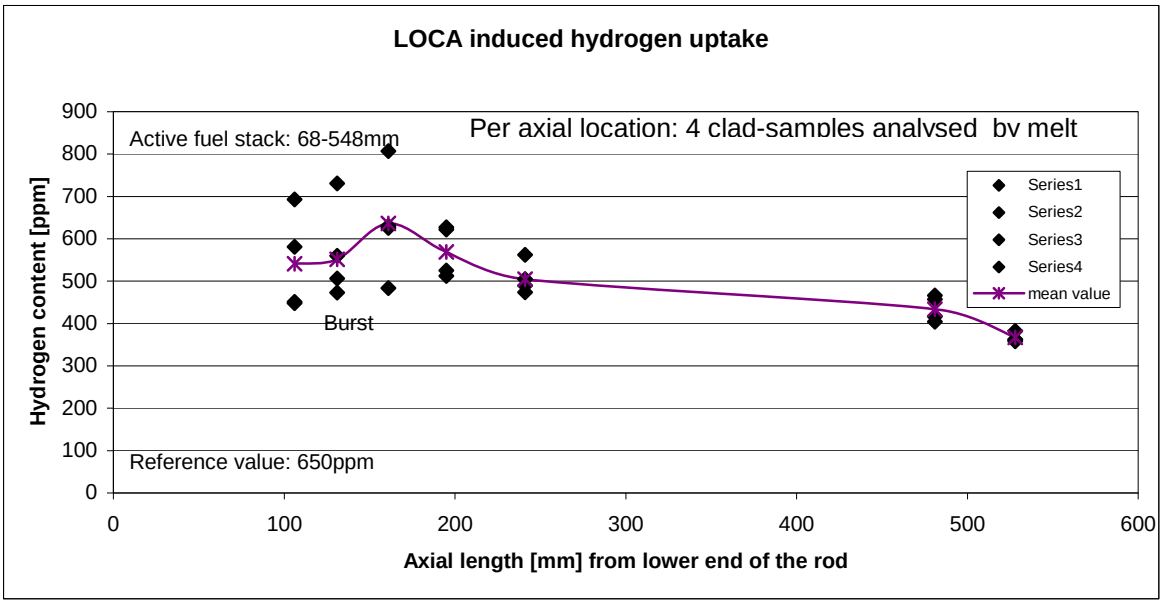

Fig. 7 Typical arbitrary oriented hydrides in the Widmanstätten structure of the cladding as seen in a cross-section from the balloon zone. The LOCA induced hydrogen uptake is illustrated in the hydrogen content profile measured along the axial length of the rod.

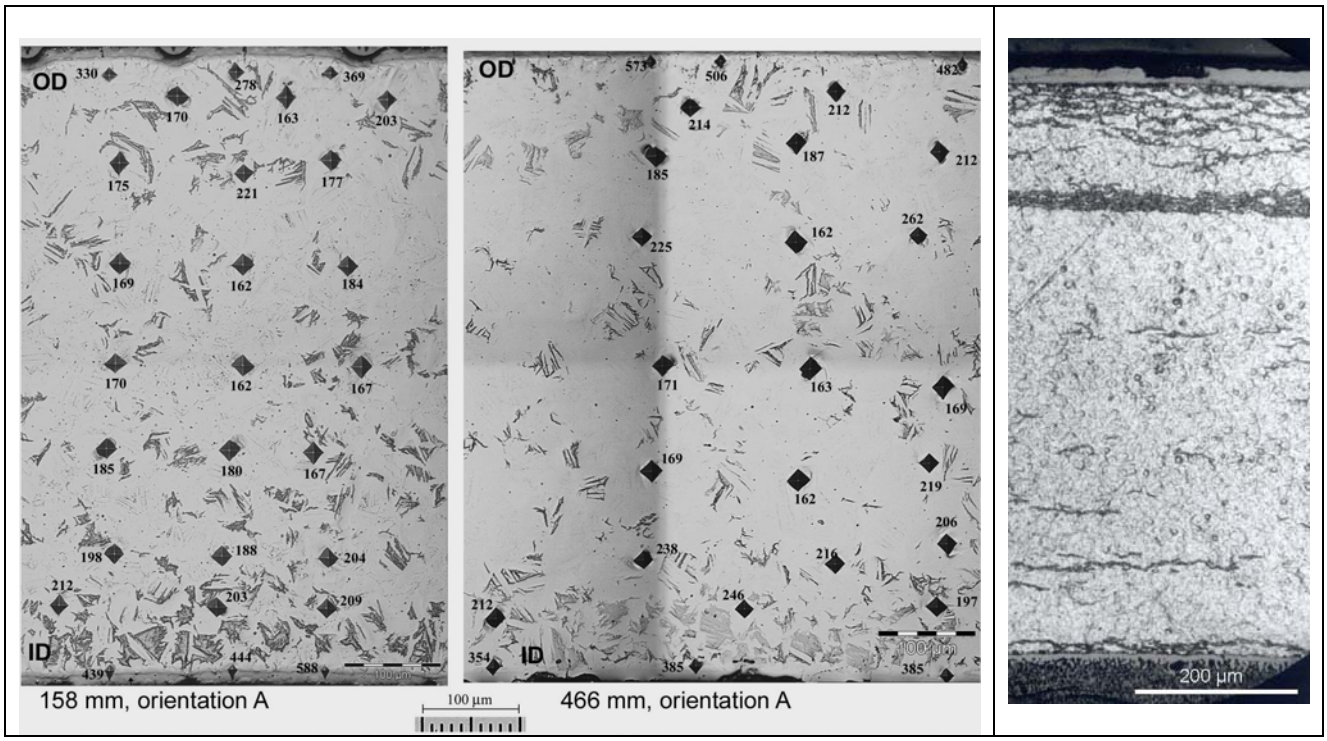

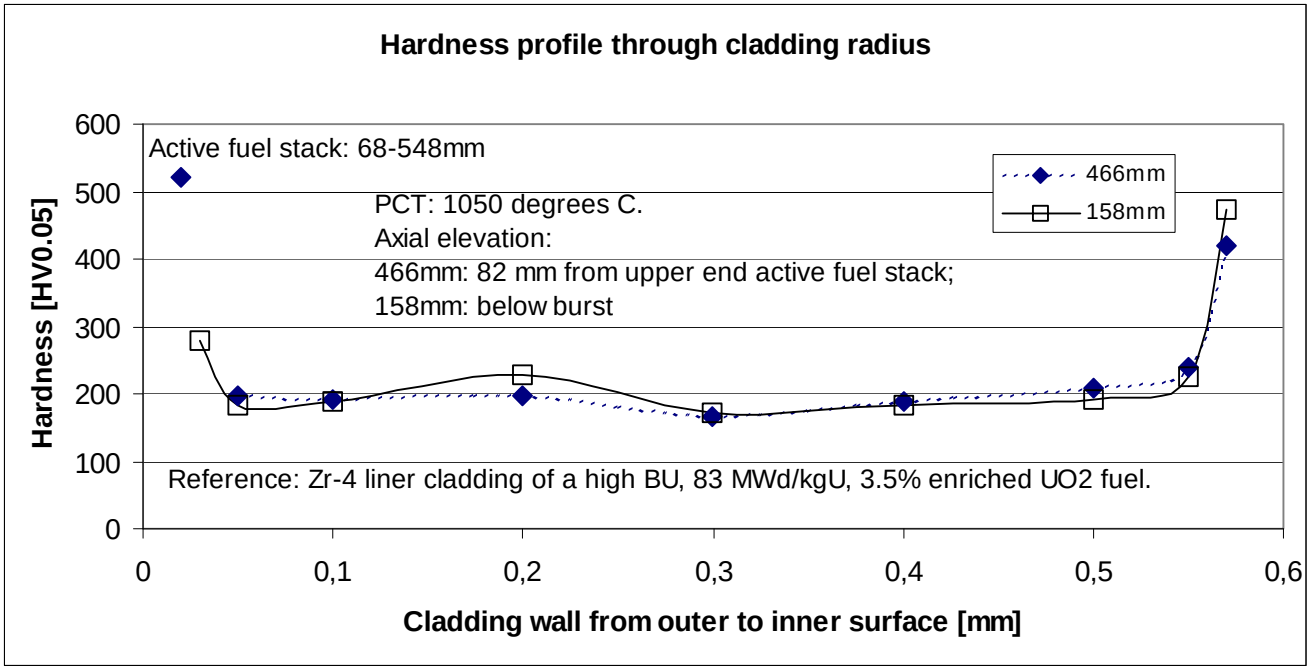

Fig. 8 Hydrides (right: before (reference PIE) and left: after LOCA), hardness indents and profile in cladding radius. Sampling locations were towards the upper end active fuel stack (466 mm) and above the upper end burst [158mm]

Table 2 Hardness measurements in IFA-650-5 with a Vickers diamond indentor and 50 g load.

Axial position 158 mm

Radial position, mm, from outer surface	**Orientation A measurements HV0,05**	**average HV0,05**	**Orientation B measurements HV0,05**	**average HV0,05**	**Average HV0,05 orientation A+B**
1)Outer surface	330, 278, 369	326	289, 221, 194	235	**280**
2) 0,05	170, 163, 203	170	216, 172, 207	198	**184**
3) 0,1	175, 221, 177	191	178, 189, 204	190	**190**
4) 0,2	169, 162, 184	172	184, 194, 184	281	**227**
5) 0,3	170, 162, 167	177	169, 162, 176	169	**173**
6) 0,4	185, 180, 167	177	198, 176, 191	188	**183**
7) 0,5	198, 188, 204	197	192, 171, 191	185	**191**
8) 0,55	212, 203, 209	208	262, 242, 228	244	**226**
9) Inner surface	439, 444, 588	490	393, 505, 476	458	**474**

Axial position 466 mm

Radial position, mm, from outer surface	**Orientation A measurements HV0,05**	**average HV0,05**	**Orientation B measurements HV0,05**	**average HV0,05**	**Average HV0,05 orientation A+B**
1)Outer surface	573, 506, 482	520	531, 531, 512	525	**522**
2) 0,05	214, 212,	213	175, 189, 187	184	**198**
3) 0,1	185, 187, 212	195	203, 203, 154	187	**191**
4) 0,2	225, 162, 262	216	194, 176, 159	176	**196**
5) 0,3	171, 163, 169	168	163, 165, 163	164	**166**
6) 0,4	169, 162, 219	183	191, 218, 173	195	**189**
7) 0,5	238, 216, 206	220	195, 200, 195	197	**208**
8) 0,55	212, 246, 197	218	286, 269, 221	259	**239**
9) Inner surface	354, 385, 385	375	506, 420, 470	465	**420**

Cladding distension (hoop strain), wall thickness reduction and crack opening: Data for the mechanical properties of the cladding e.g. cladding distension (hoop strain), wall thickness reduction and crack opening were measured and are listed in Table 3 and plotted as axial profiles in Fig.9.

The cladding diameter measurements on IFA-650.5 show a relatively small strain in the rupture region, but they also show a relatively large strain along almost the whole length of the test specimen.

Table 3 Cladding distension (Hoop strain), wall thickness reduction

Axial position (mm)	*** Cladding circumference (mm)**	**# Cladding diameter (mm)**	**¤ Cladding wall thickness (mm)**
95 (MC1)	34.79	11.72	0.566
120 (MC2)	35.06	11.815	0.579
150 (MC3)	34.87	11.909	0.581
184 (MC4)	34.55	11.722	0.594
230 (MC5)	33.79	11.363	0.596
470 (MC6)	33.03	11.094	0.621
517 (MC7)	32.41	11.036	0.651

* measured on macrographs at half wall thickness
# measured on macrographs – average from 3 orientations
¤ mean value of 8 measurements on clad circumference

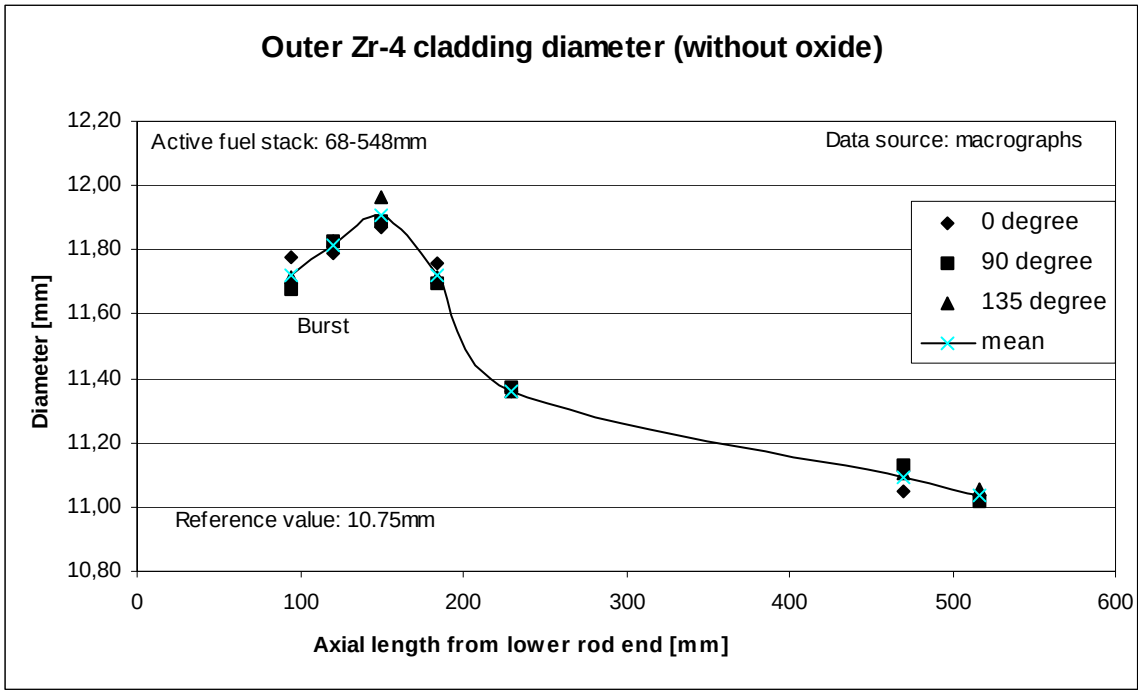

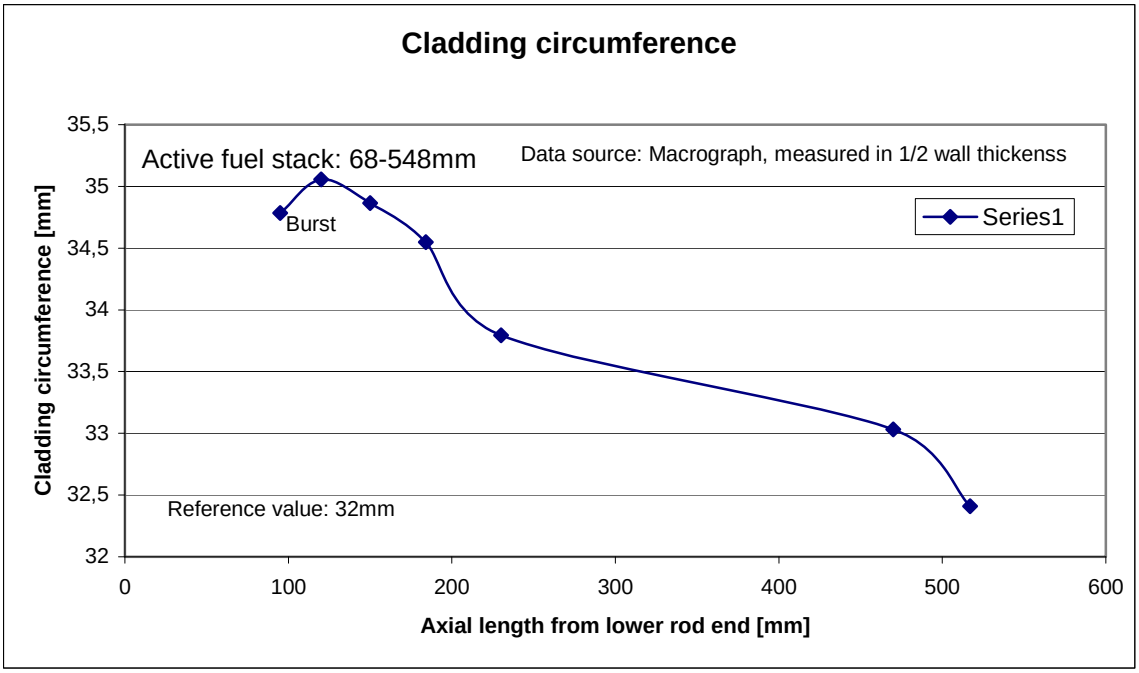

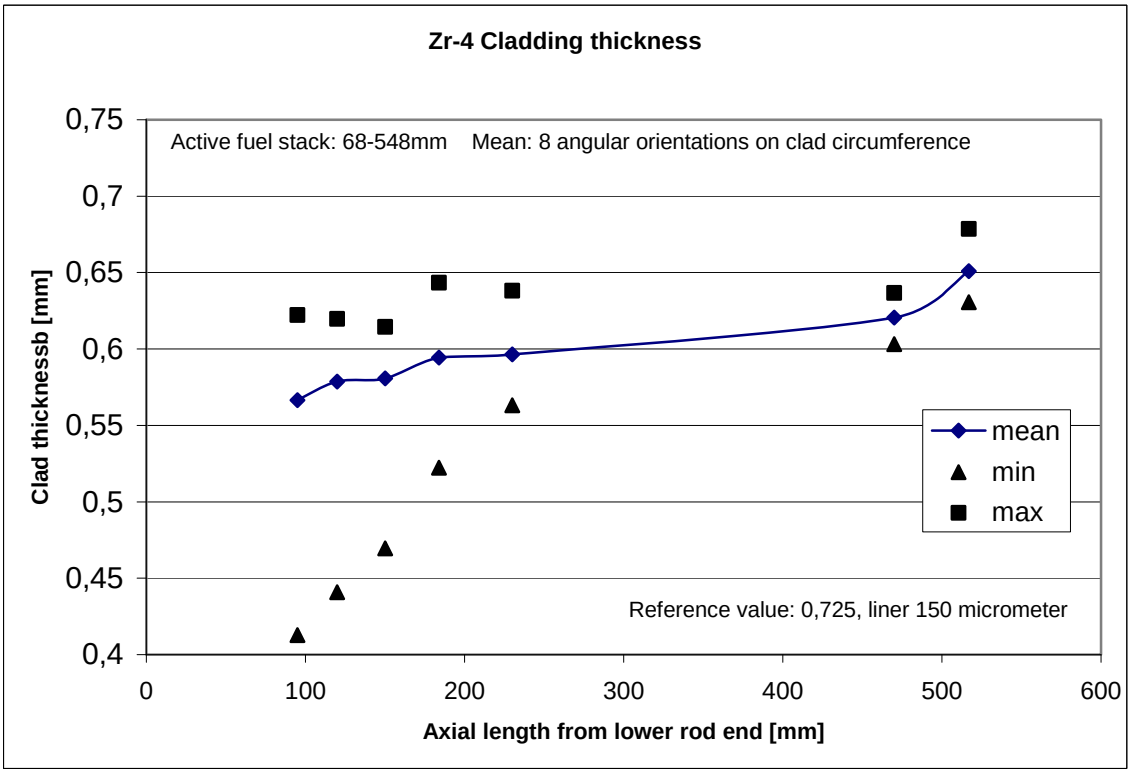

Fig 9. Axial profiles for diameter increase, cladding circumference (Hoop strain profile), cladding thickness / wall reduction.

3.5.2 Fuel-clad bonding

Fuel-clad bonding, radial cracks in ID oxide and in the fuel rim were observed, see Fig 10. The fuel had typically a fragmented HBU rim structure, characterized by micrometer size pores, sub-micrometer grains.

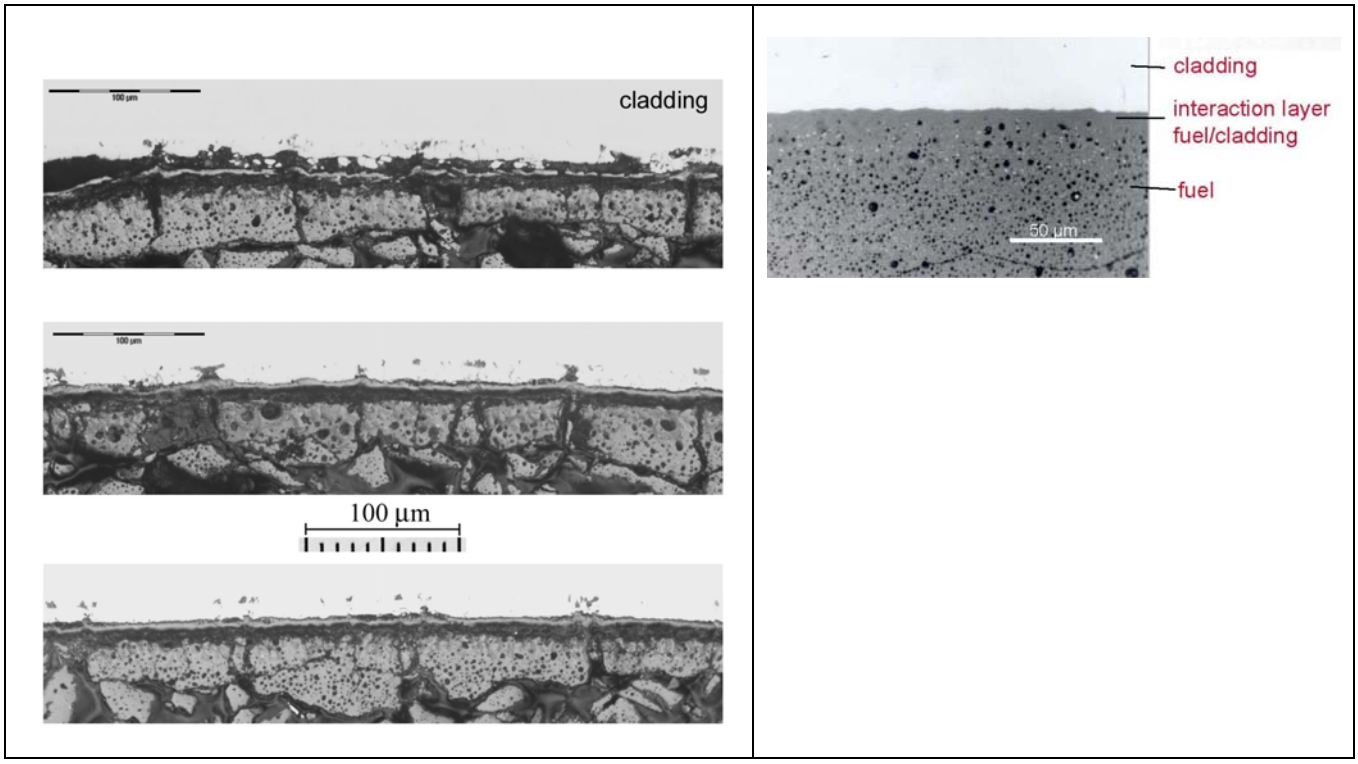

Fig. 10 Fuel-clad bonding. The cladding ID shows radial cracked oxide and fuel with fragmented HBU rim structure. The fragments are typically elongated (right). Pre-test reference PIE (left).

4 Summary and Conclusion

The 83 MWd/kg PWR rod segment used in rod 650-5 reached a PCT of 1050 °C in the LOCA test. The rod segment had 3.5 % enriched UO_2 fuel and a Zr-4 cladding with an outer diameter (OD) liner. The high burn-up PWR segment showed LOCA induced ballooning with a burst at 7-8 cm above the lower end active fuel stack and well below the lower cladding thermocouple. The burst opening is about 1 cm long and narrow.

The rod showed a surface oxide layer with radial cracks going in longitudinal direction. The cladding diameter measurements on IFA-650.5 showed, a relatively small strain in the rupture region, but they also showed a relatively large strain along almost the whole length of the test specimen. The burst opening and the balloon size observed towards the lower end of the rod indicated a less ductile cladding, compared to rod 650-4 due to the high hydrogen content.

Neutronradiographs from the upper part of the rod revealed pellets in tight contact with the cladding and pellet cracks, and in the lower part cladding distension and fuel fragmentation was measured.

Metallography cross-sections from the burst region, namely 7 mm above and 23 mm below the max balloon, showed on the cladding a continuous, 70 mm thick oxide on the outer diameter. Radial cracks in the cladding outer and inner diameter oxide were seen. In the balloon the cladding contained up to 800 ppm hydrogen, and showed an oxide growth of up to 13 micrometer. The hydrogen rich cladding microstructure showed Widmanstätten structure (former β-grains) and grain growth to a gain-size of about 40 μm. A hard and brittle alpha layer is found on outer cladding diameter. Further, the IFA-650.5 test exposed the high-burnup fuel rod to appropriate LOCA conditions, and microscopic examination had confirmed, as expected from early work on cladding embrittlement by oxygen ingress into the cladding, the presence of an alpha phase structure in a layer near the cladding ID. The alpha layer is slightly wider on the inner diameter (ID) compared to the outer (OD) and the alpha layer is wider in the max balloon and burst area (OD:24 and ID:29 μm) compared to the upper part of the rod at 470 mm (OD:20 and ID:22 μm). The oxygen necessary for the ID alpha layer formation in the upper part of the rod originated from the bonded fuel. The hardness of the high burnup, LOCA tested Zr-4 cladding showed in the balloon zone throughout the cladding radius hardness values within 170 and 200 HV_{100}. A slight hardness increase was seen near the OD in the range of the liner.

Appendix

Cladding as fabricated.

Reference data by the supplier.

Rod identification		V1-515
Cladding typ		DX ELS0.8b
Base material Zry-4	chemical composition	
	Sn %	1.48
	Fe %	0.23
	Cr %	0.12
Outer liner	chemical composition	
	Sn %	0.84
	Fe %	0.29
	Cr %	0.17
	Nb %	-
Final heat treatment		stress relief anneal
Outside diameter	mm	10.735
Inner diameter	mm	9.293
Wall thickness	mm	0.725 (nom)
Liner thickness	mm	0.15 (nom)
Mechanical properties	RT	400°C
0.2 yield strength $R_pO.2$; N/mm2	574	317
Tensile strength R_m; N/mm2	754	400
Elongation As; %	17.7	22.5
Constant bursting elongation; %	-	5.1

Cladding prior to LOCA.

Reference PIE by the supplier.

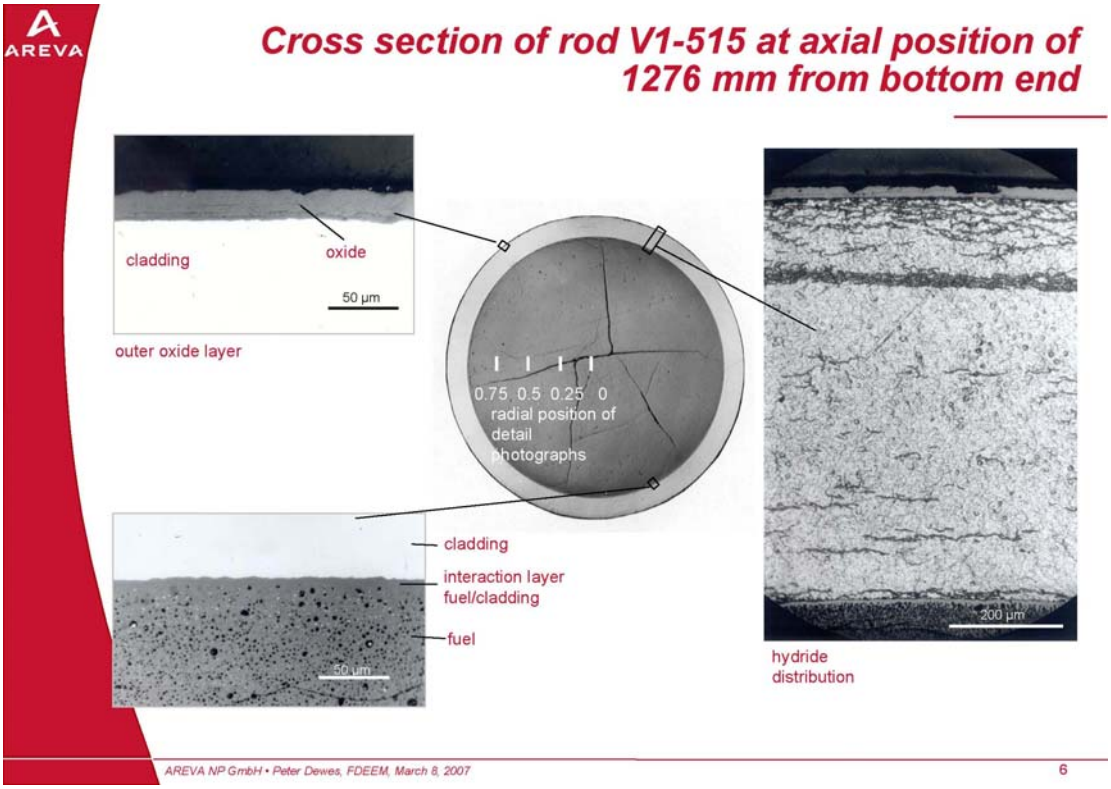

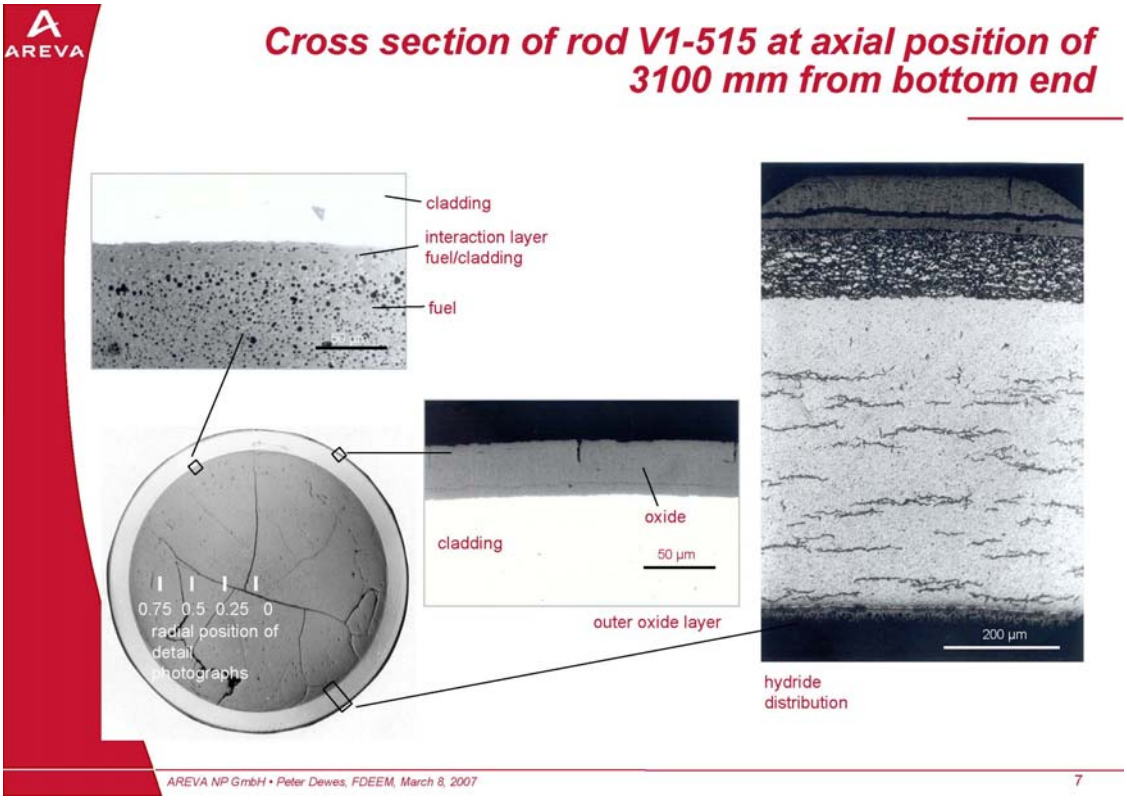

Alpha layer – supplementary Figures

Fig. 3.5.18 through 3.5.24

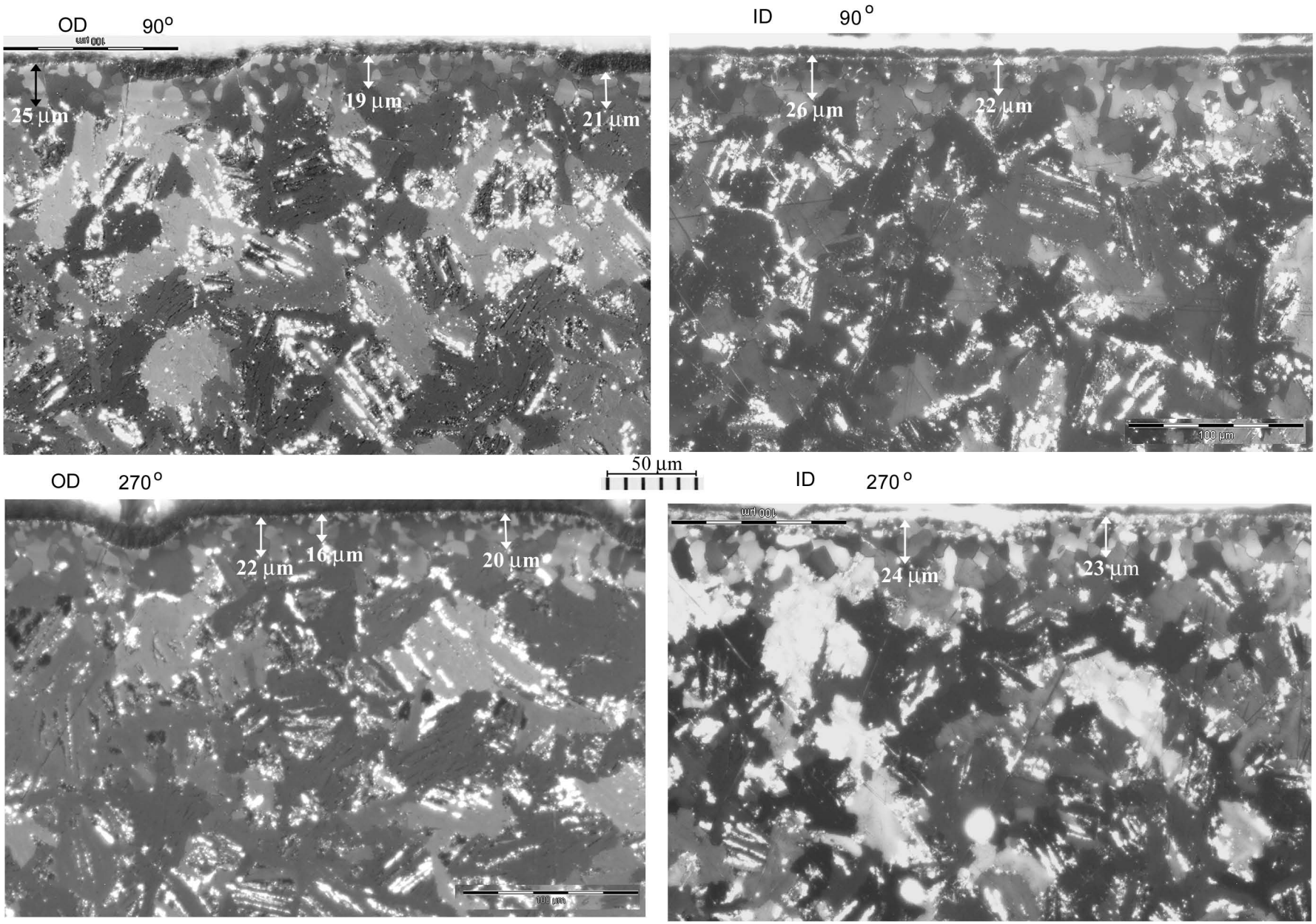

Fig. 3.5.18. Details showing the grain morphology of cladding and alpha layer on outer (OD) and inner (ID) surface. IFA-650-5 at axial position 95 mm (MC1) from lower end of fuel rod.

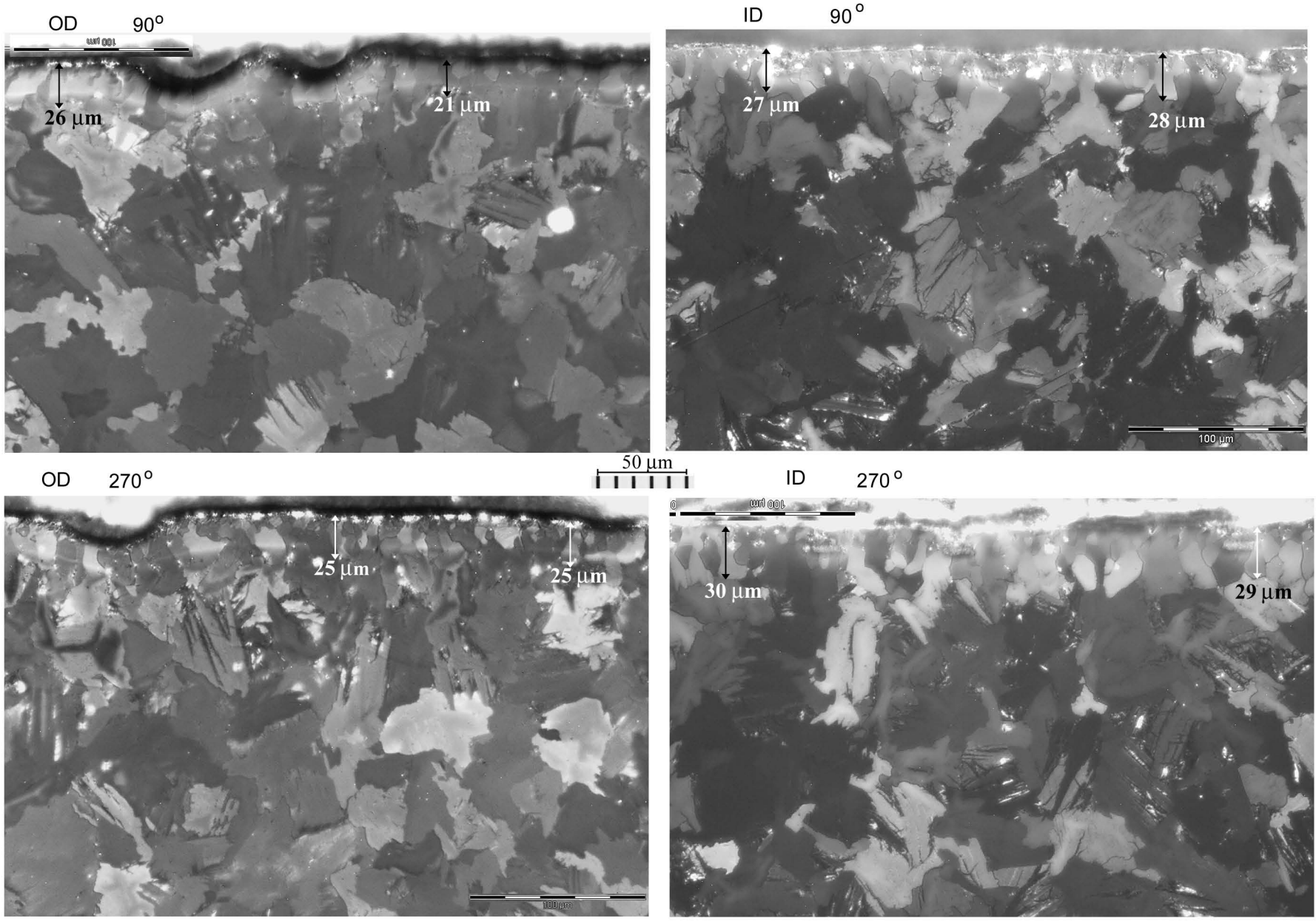

Fig. 3.5.19. Details showing the grain morphology of cladding and alpha layer on outer (OD) and inner (ID) surface. IFA-650-5 at axial position 120 mm (MC2) from lower end of fuel rod.

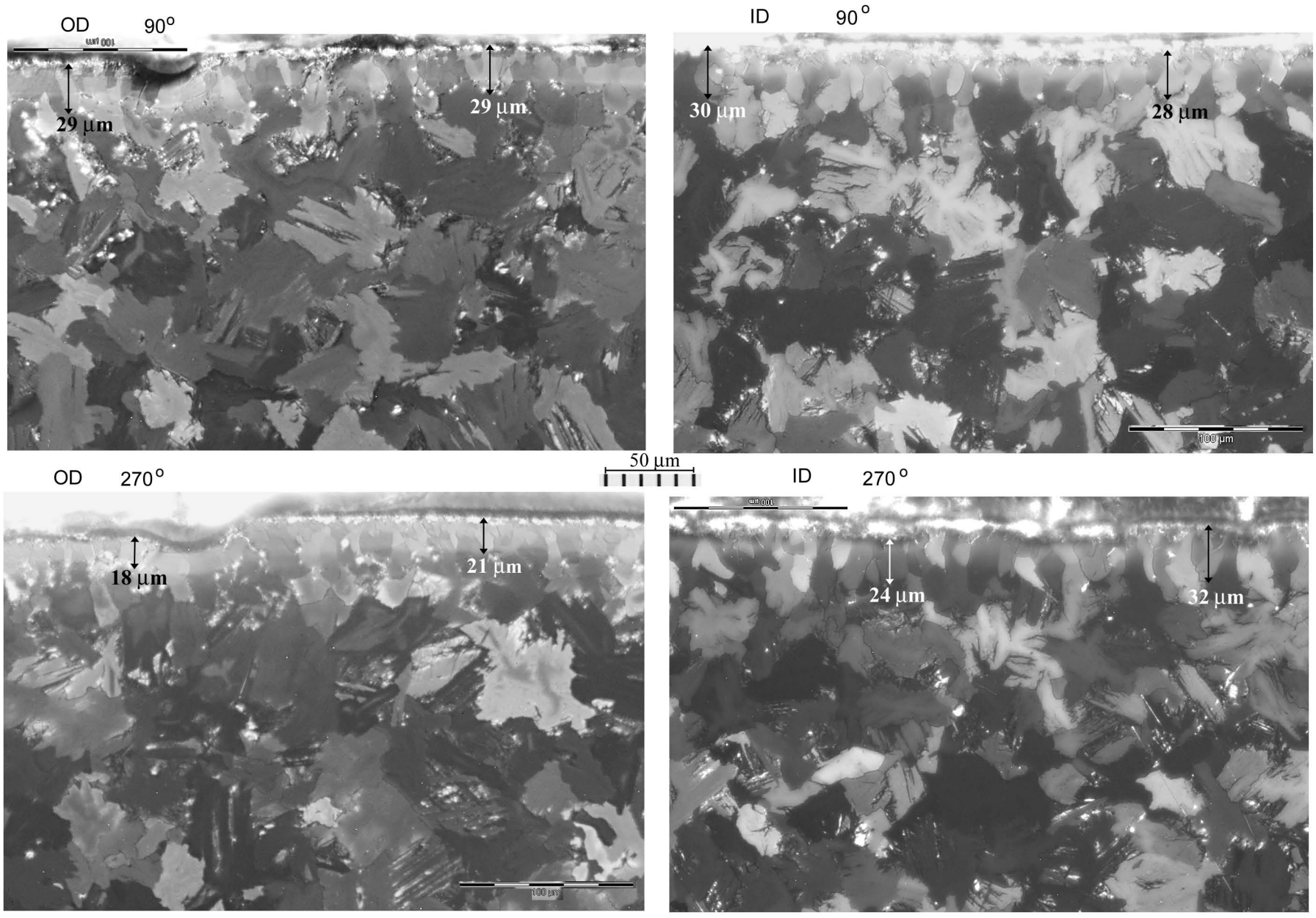

Fig. 3.5.20. Details showing the grain morphology of cladding and alpha layer on outer (OD) and inner (ID) surface. IFA-650-5 at axial position 150 mm (MC3) from lower end of fuel rod.

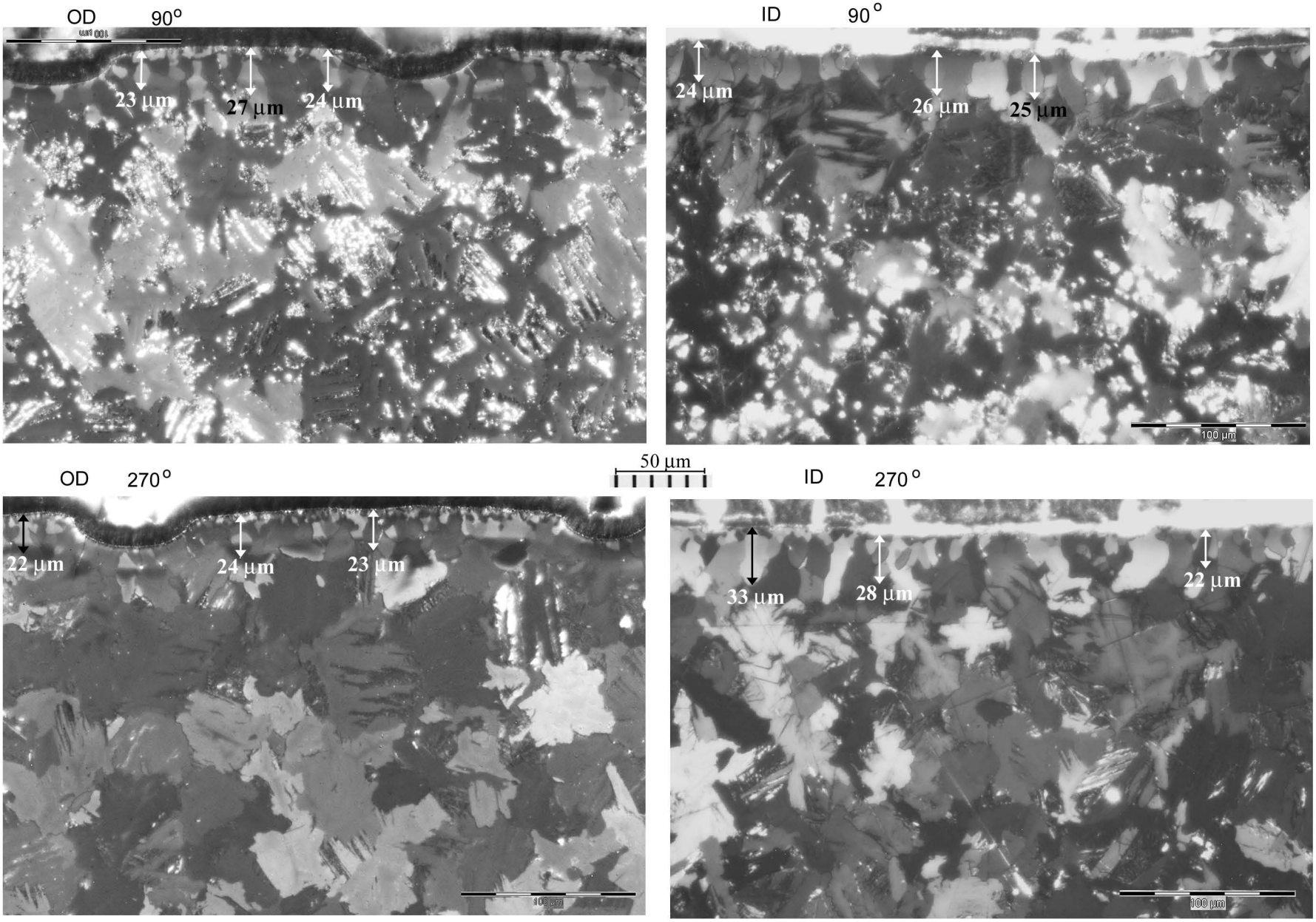

Fig. 3.5.21. Details showing the grain morphology of cladding and alpha layer on outer (OD) and inner (ID) surface. IFA-650-5 at axial position 184 mm (MC4) from lower end of fuel rod.

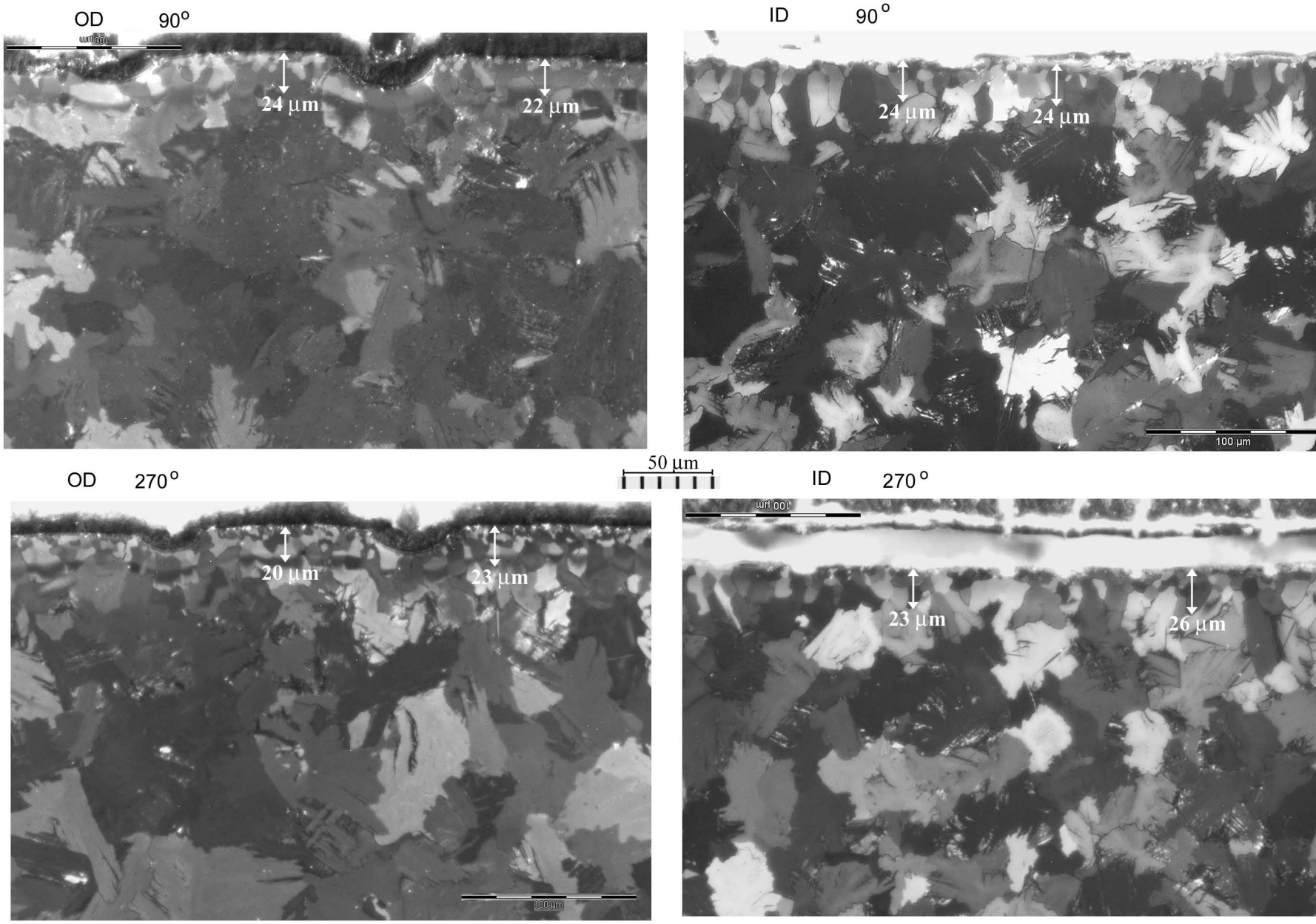

Fig. 3.5.22. Details showing the grain morpholoy of cladding and alpha layer on outer (OD) and inner (ID) surface. IFA-650-5 at axial position 230 mm (MC5) from lower end of fuel rod.

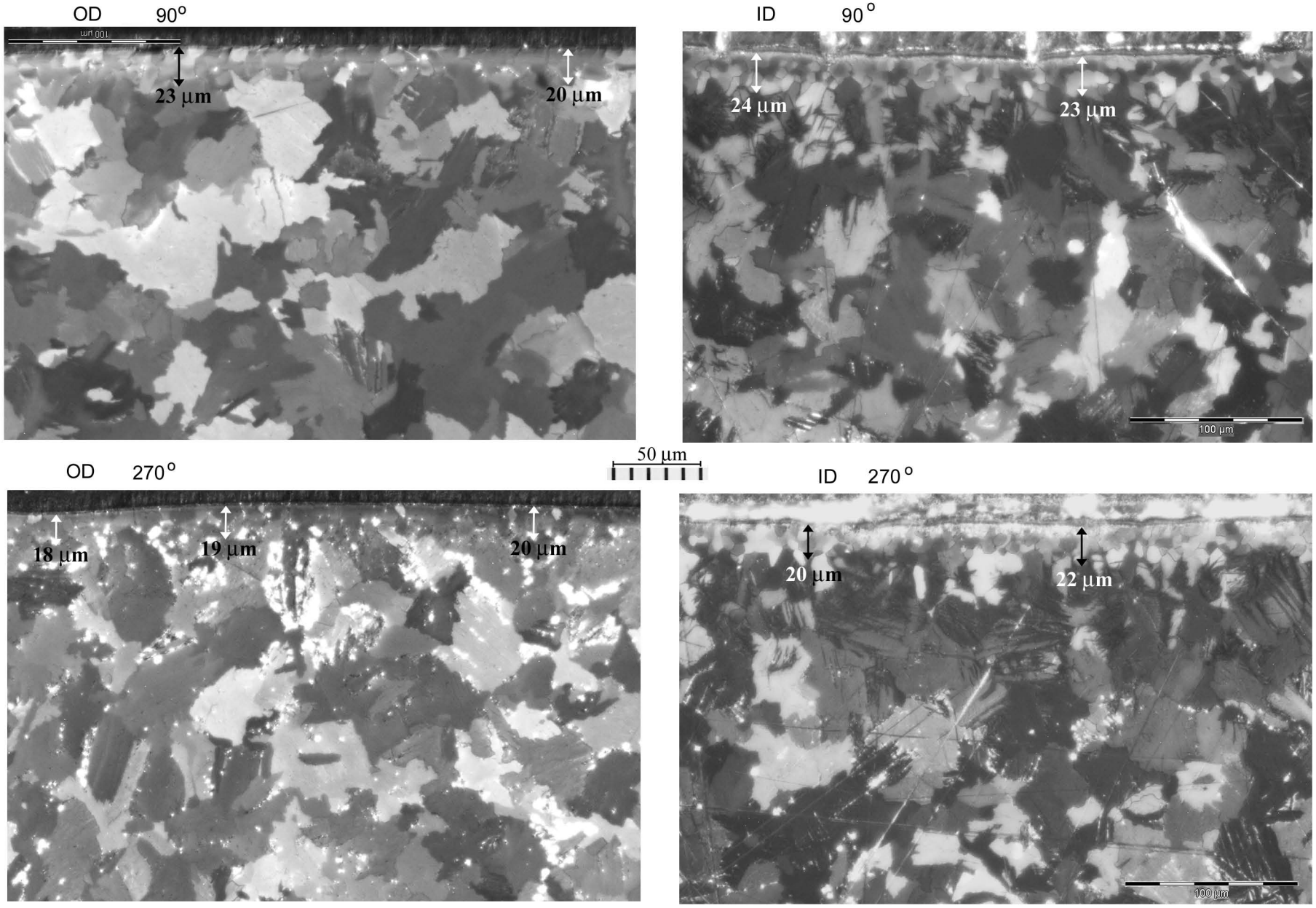

Fig. 3.5.23. Details showing the grain morphology of cladding and alpha layer on outer (OD) and inner (ID) surface. IFA-650-5 at axial position 470 mm (MC6) from lower end of fuel rod.

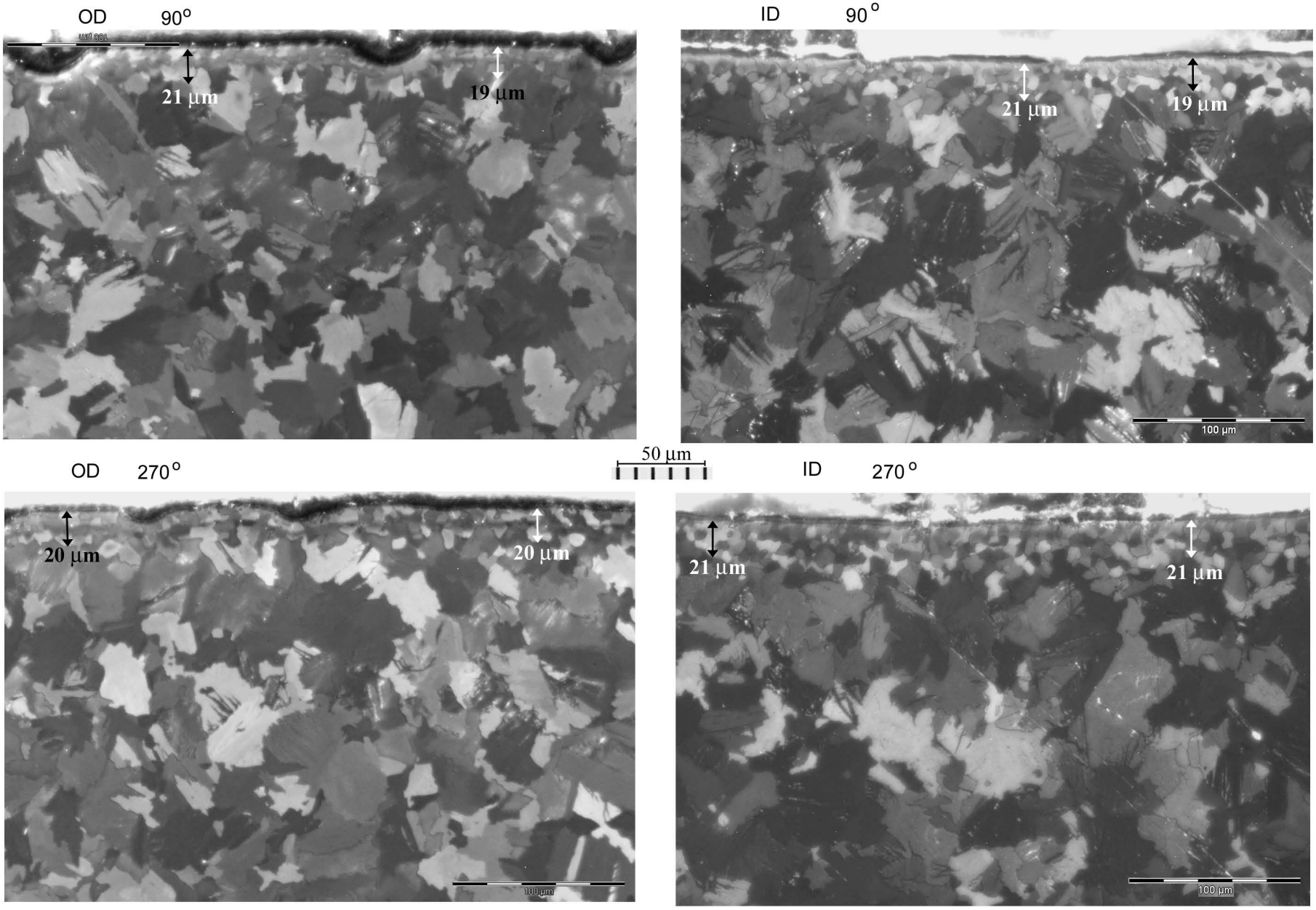

Fig. 3.5.24. Details showing the grain morphology of cladding and alpha layer on outer (OD) and inner (ID) surface. IFA-650-5 at axial position 517 mm (MC7) from lower end of fuel rod.

Hardness data – supplementary Figures

Fig. 3.5.32 through 3.5.35

Hardness measurements - Vickers diamond indenter - load 50 gf

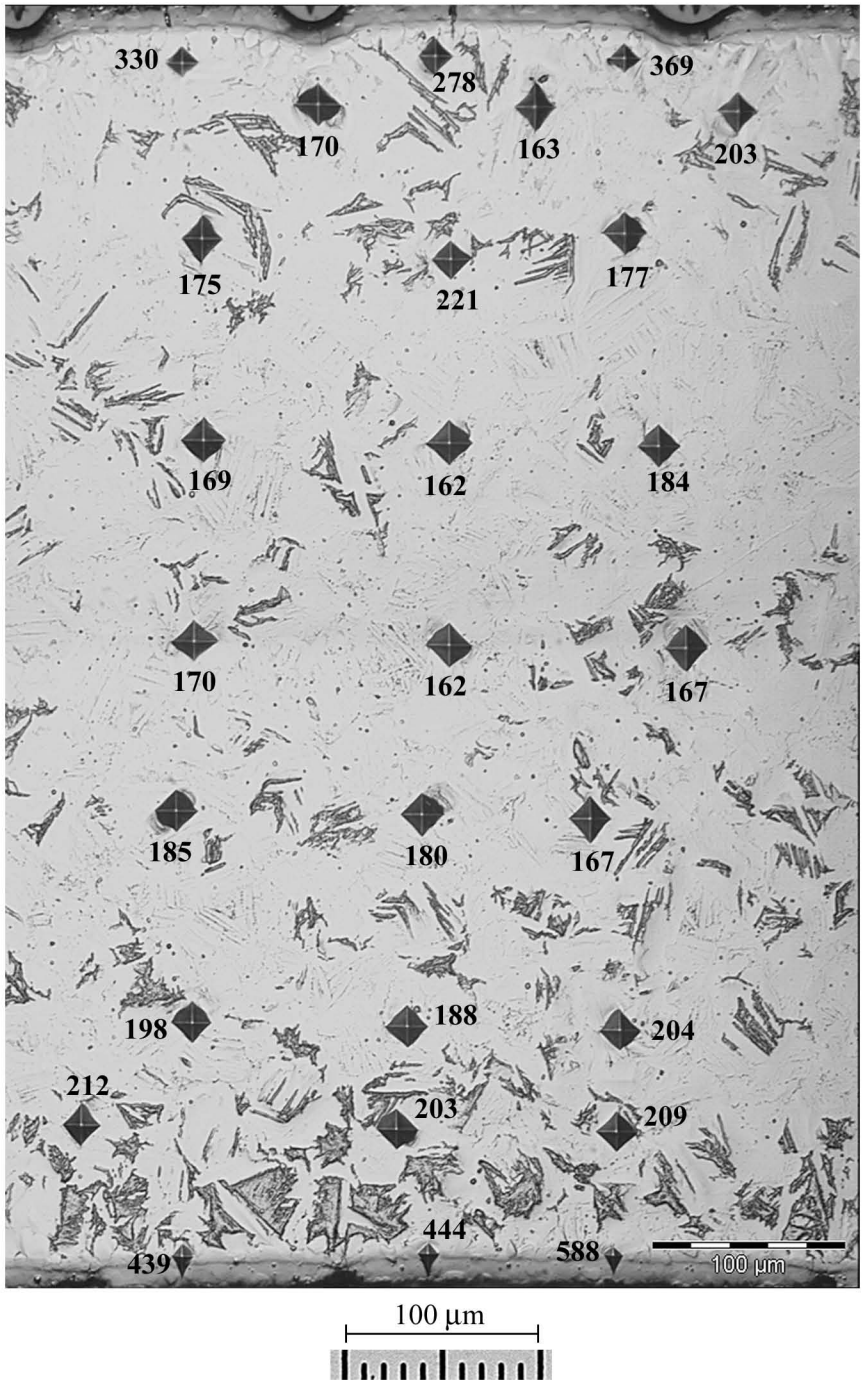

Fig. 3.5.32. Hardness measurement (HV0.05) of IFA-650-5 at orientation A and axial position 158 mm from lower end of fuel rod in etch-polished condition.

Hardness measurements - Vickers diamond indenter - load 50gf

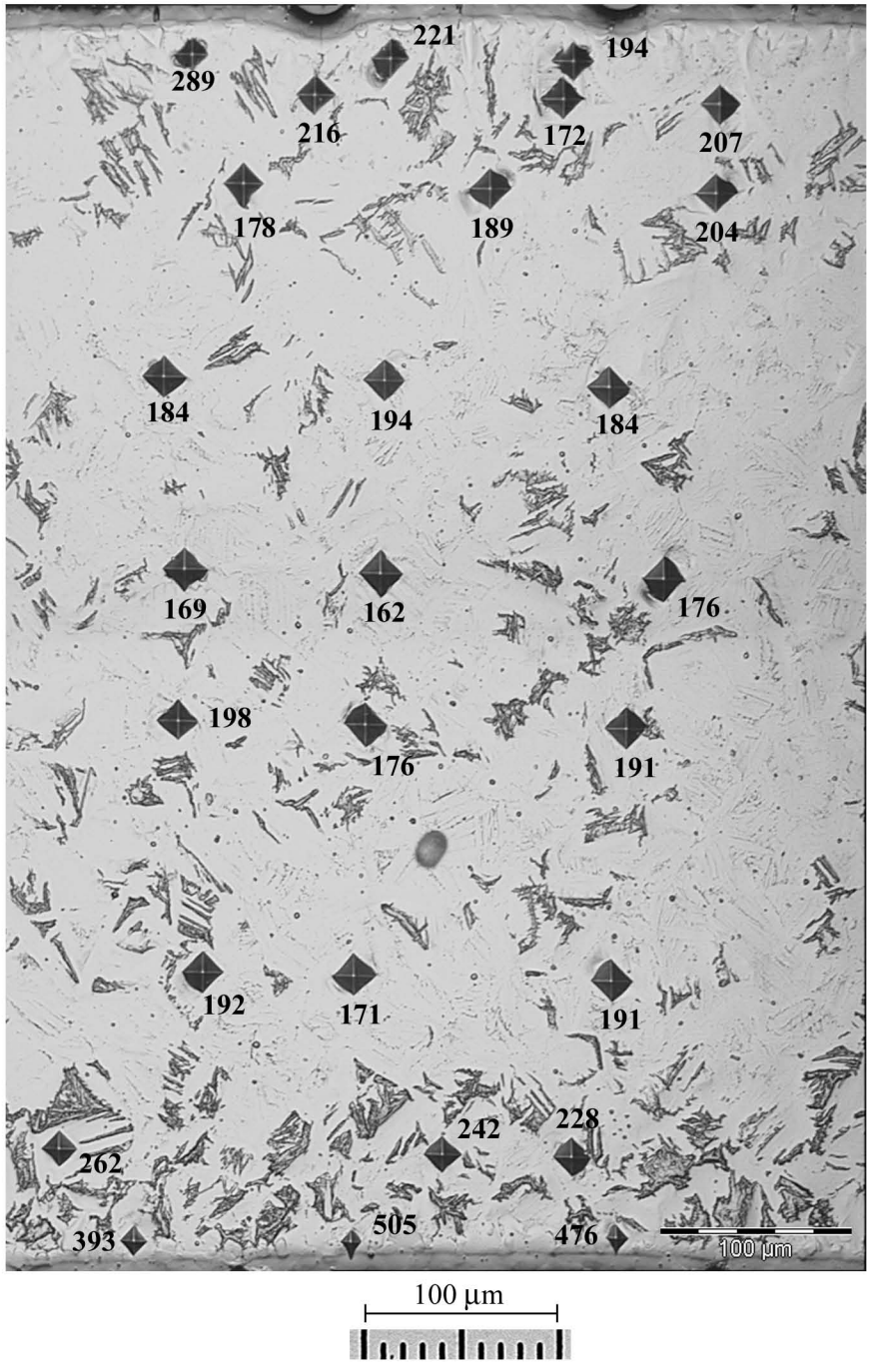

Fig. 3.5.33. Hardness measurement (HV0.05) of IFA-650-5 at orientation B and axial position 158 mm from lower end of fuel rod in etch-polished condition.

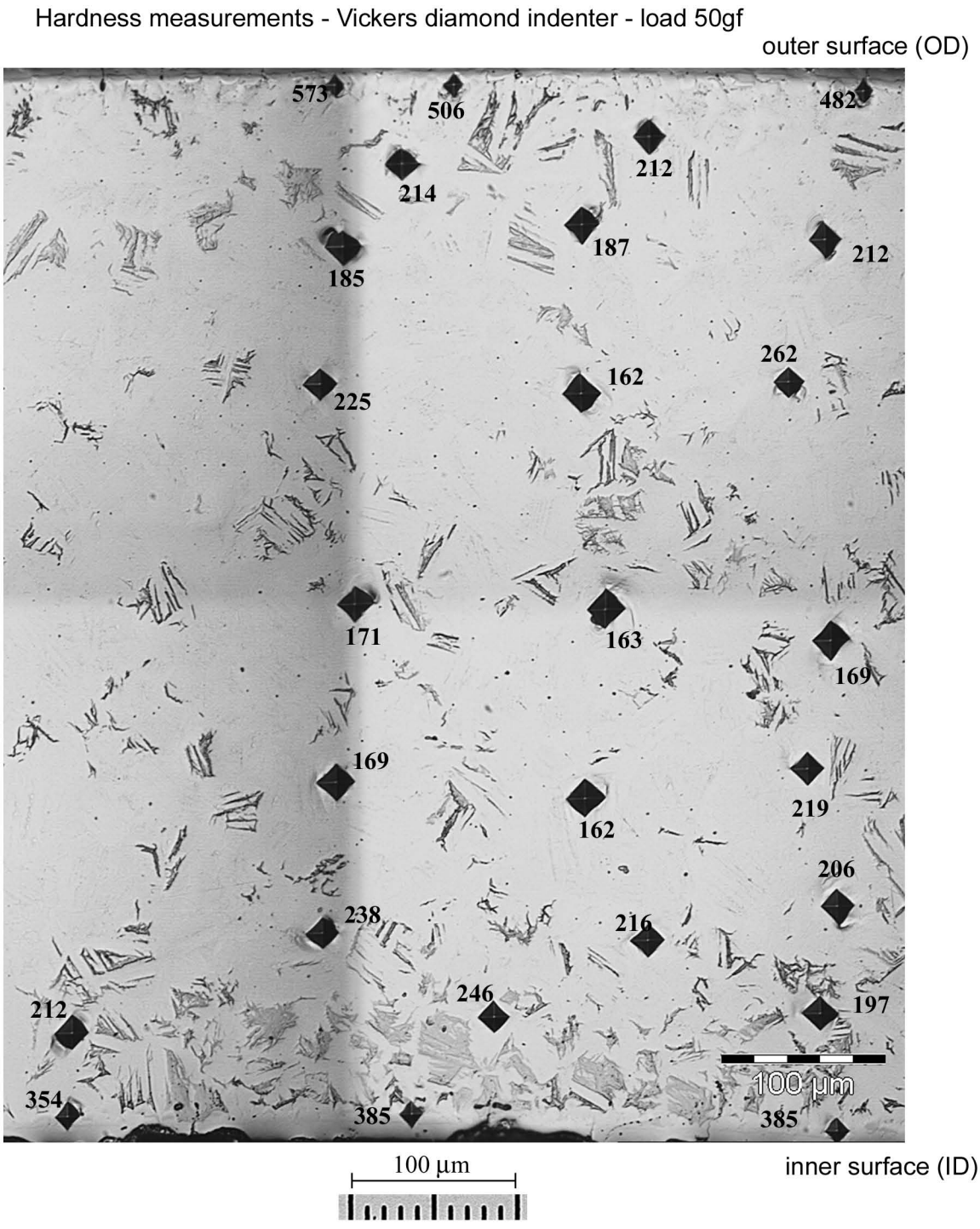

Fig. 3.5.34. Hardness measurement (HV0.05) of IFA-650-5 at orientation A and axial position 466 mm from lower end of fuel rod in etch-polished condition.

Hardness measurements - Vickers diamond indenter - load 50gf

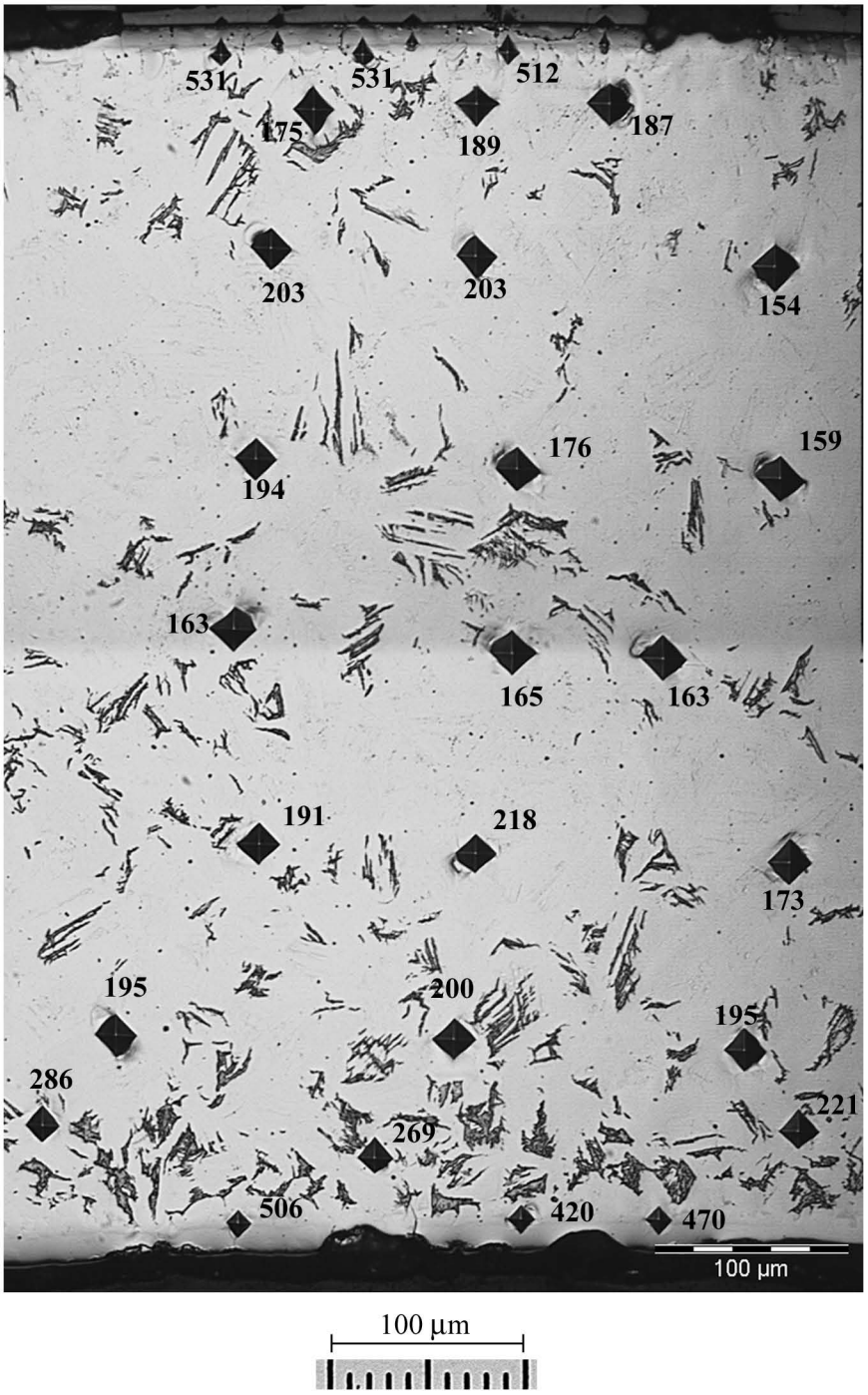

Fig. 3.5.35. Hardness measurement (HV0.05) of IFA-50-5 at orientation B and axial position 466 mm from lower end of fuel rod in etch-polished condition.